Molecular Mechanisms of Antiviral Effect of Interferon and Host Response to Hepatitis C Virus Infection

A Dissertation Submitted to
the Graduate School of Life and Environmental Sciences,
the University of Tsukuba
in Partial Fulfillment of the Requirements
for the Degree of Doctor of Philosophy in Biological Science
(Doctoral Program in Biological Sciences)

Hideyuki KONISHI

Table of contents

Abstract

Introduction and Aim

Most acute Hepatitis C virus (HCV) infections become chronic, with some progression to liver cirrhosis or hepatocellular carcinoma (HCC). Current therapy against chronic HCV infection includes pegylated interferon (PEG-IFN)-α, which achieves a sustained virological response in only 50% of patients. IFN-α induces JAK/STAT activation and subsequent antiviral genes (IFN-stimulated genes, ISG) expression. Clinically, hepatic ISG expression is known to be associated with the efficacy of IFN therapy. Recently, a genome-wide association study showed that single nucleotide polymorphisms (SNPs), located near interleukin (IL)28B, are strongly associated with a virological response to IFN therapy. IL28B SNP was reported to associate with ISGs expression, although, the mechanism underlying the association was unclear.

The main causes of low response by IFN therapy may be (i) low compliance with the therapy, which must be administered subcutaneously, costs and the side effects of IFN, and (ii) poor prediction of clinical outcomes with IFN therapy. To overcome these problems, an orally available small molecule IFN would be valuable, and association between IL28B SNP and ISG

expressions is elucidated.

Methods

Chapter 1: Using HCV replicon harboring cells, a high-throughput screening was performed to identify HCV inhibitors. The induction of gene expression, especially ISGs, and JAK/STAT phosphorylation by RO8191 treatment in the replicon cells were detected. RO8191 activity in the cells that were knocked down IFN signaling molecules was evaluated. RO8191 activity in IFN receptor-deficient cells was also analyzed. I administered orally RO8191 to mice and detected gene expression in the mice liver. I also administered RO8191 to HCV infected humanized liver chimeric mice and measured HCV viral titer.

Chapter 2: Data were collected from 74 patients with HCV-induced hepatocellular carcinoma. The IL28B genotype and hepatic ISG mRNA levels were analyzed to clarify their association, focusing on the progression of liver fibrosis.

Results

Chapter 1: I identified an orally available, small-molecule type I IFN receptor agonist (RO8191) that directly transduces the IFN signal cascade and stimulates antiviral gene expression. Like type I IFN, the small-molecule compound induces ISG expression for antiviral

activity *in vitro* and *in vivo* in mice, and the ISG induction mechanism is attributed to a direct interaction between the compound and IFN-α receptor 2, a key molecule of IFN-signaling on the cell surface.

Chapter 2: Hepatic ISG15 expression was lower in the IL28B major (rs8099917 TT) group than that in the IL28B minor (rs8099917 TG or GG) group. IFN γ-induced protein-10 (IP-10) expression was similar between the IL28B major and minor groups. IP-10 expression was elevated with advancing stages of liver fibrosis in HCV-infected patients. In patients with mild or no fibrosis, the IL28B major group had lower IP-10 expression than the IL28B minor group. However, in patients with advanced fibrosis, IP-10 expression was not different between the IL28B major and minor groups.

Conclusions

RO8191 is a novel small molecule that activates IFN signaling directly, and the host response to hepatitis C virus infection, focusing on the association among IL28B SNP, IP-10 expression, other ISG expression and liver fibrosis, is analyzed.

RO8191 would contribute a development of novel treatment to chronic hepatitis C patients even with IL28B unfavorable genotype.

Abbreviations

γ-GTP, γ-glutamyl transpeptidase

ALT, alanine aminotransferase

ANOVA, Analysis of variance

BMI, body mass index

DAB, 3,3' -diaminobenzidine tetrahydrochloride

DMEM, Dulbecco's modified Eagle's medium

ECD, Extracellular domain

EMCV, Encephalomyocarditis virus

FBS, Fetal bovine serum

FCS, Fetal calf serum

GAPDH, Glyceraldehyde 3-phosphate dehydrogenase

HCC, Hepatocellular carcinoma

HCV, Hepatitis C virus

HTS, High-throughput screening

KO, Knockout

IC_{50}, 50% inhibitory concentration

IFN, Interferon

IFNAR, IFN-α receptor

IL, Interleukin

IP-10, IFN γ-induced protein-10

ISG, IFN-stimulated genes

ISGF3, IFN-stimulating gene factor 3

ISRE, IFN-stimulated response element

MEF, Mouse embryonic fibroblasts

NBNC, Non-B, non-C

NEAA, Non essential amino acid

NS, Nonstructural

PEG, Pegylated

RBV, Ribavirin

RT-PCR, Reverse transcription-polymerase chain reaction

SCID, Severe combined immunodeficient

SNP, Single nucleotide polymorphisms

SP, Sodium pyruvate

SPR, Surface plasmon resonance

STAT, Signal transducers and activators of transcription

SVR, Sustained virological response

TLR, Toll-like receptor

TNF, Tumor necrosis factor

General Introduction

Hepatitis C virus (HCV) infection affects 170 million people worldwide [41], and most acute HCV infections become chronic, with some progression to liver cirrhosis or hepatocellular carcinoma (HCC). HCV has a plus-strand RNA genome that encodes both structural proteins and the nonstructural (NS) proteins 2, 3, 4A, 4B, 5A and 5B. HCV infection induces Interferon (IFN) production via innate immune cascades [47, 65]. IFN consists of type I (IFN-α, β, and others), II (only IFN-γ), and III (IFN-λs; interleukin, or IL28A/B and IL29) IFNs. IFNs induce the expression of a subset of IFN-stimulated genes (ISG) [71, 72], some of which show antiviral activity or are involved in lipid metabolism, apoptosis, protein degradation and inflammation [10]. Broadly speaking, type I IFNs bind to their receptor, causing the phosphorylation and activation of JAK1 and Tyk2, which is followed by the phosphorylation of signal transducers and activators of transcription (STATs) and subsequent ISG expression. To activate the JAK/STAT pathway, IFN-α requires the IFN-α/β receptor, which consists of 2 subunits, IFN-α receptor (IFNAR) 1 and IFNAR2. These IFNAR subunits together form a heterodimer upon IFN stimulation. This association of IFNAR2 and IFNAR1 is required to mediate the antiviral, antiproliferative, and apoptotic effects of type I IFNs [53, 58, 80], because

the dimerization of IFNARs induces the phosphorylation of the receptor-associated tyrosine kinases, JAK1 and Tyk2, and the phosphorylated JAK kinases then phosphorylate STAT1 and STAT2. In turn, phosphorylated STAT1 and STAT2 bind to IRF9 to form the transcriptional activator IFN-stimulating gene factor 3 (ISGF3) that induces the expression of a subset of ISGs.

Current standard therapy against chronic HCV infection includes the use of host factor-targeting pegylated (PEG) IFN-α and ribavirin (RBV) [19], which achieve a sustained virological response (SVR) in only 50% of patients chronically infected with the HCV genotype 1 [17, 50, 85]. The main causes of this low rate of efficacy may be (i) low compliance with the therapy, which must be administered subcutaneously, and (ii) poor prediction of clinical outcomes with IFN therapy.

Regarding the lack of compliance, the current therapy using recombinant IFN is a weekly injectable formulation that is unstable, requires refrigeration, and is expensive and complex to administer. Furthermore, therapy is often poorly tolerated as a result of the presence of many adverse effects, including flu-like symptoms, hematological abnormalities and adverse neuropsychiatric events, any of which may require early discontinuation [7]. These side effects may result in dose modifications that lead to less-than-optimal responses. Recent trends in drug

development focus on drugs targeted against viral proteins such as NS 3/4A serine protease, RNA helicase, NS4B, NS5A, and NS5B RNA-dependent RNA polymerase [83]. Adding such an inhibitor to the standard therapy achieved significantly higher SVR rates, but the issue still remains that using these inhibitors without injectable IFN possibly yields clinical resistance [38]. To overcome this problem and alleviate the low compliance outlined above, an orally available IFN would be valuable because the dosing regimen is less complex. Using quantitative high-throughput screening (HTS), I identified in this study a novel small molecule that acts like IFN by directly interacting with the type I IFN receptor to drive ISG expression. My results indicate that oral administration of the small-molecule IFN agonist stimulates ISG expression in mice, and that the ISG expression from this small-molecule IFN provides antiviral activity, indicating that the compound may be a potential therapeutic IFN substitute [35].

Regarding the latter cause, the host factors that are important in the early response to therapy remain unknown, although several studies that showed an association between ISG expression and clinical outcomes with IFN have been conducted [26]. Hepatic ISG expression is known to be associated with the efficacy of IFN therapy, and high ISG expression is a predictive factor for a poor IFN response. Recently, a genome-wide association study showed

that single nucleotide polymorphisms (SNPs), located near IL28B, which encodes for IFN-λ3, are strongly associated with a virological response to IFN therapy and spontaneous clearance of HCV [18, 63, 74, 76, 77]. Especially in Japanese patients, rs8099917 is closely associated with efficacy for IFN therapy; patients with the TT genotype (termed IL28B major) have a stronger response to IFN therapy than those with TG or GG genotypes (termed IL28B minor) [76]. Even after liver resection because of HCC [32] or liver transplantation [16], the efficacy of therapy is associated with IL28B SNP. More recently, IL28B major patients were reported to express hepatic ISGs, which were lower than those in IL28B minor patients [13, 26]. However, after liver resection for HCC, the association between hepatic ISG expression and the efficacy of therapy is still unclear. IFN γ-induced protein-10 (IP-10) expression is also a predictor for IFN therapy, and high IP-10 expression is a predictive factor for a poor IFN response [39, 64]. Unlike other ISGs, serum IP-10 protein levels have been reported to be associated with differences in IL28B SNP [15, 40], and they also have been found not to be associated with differences in IL28B SNP [8]. IP-10 is one of the ISGs, and it is regulated by inflammatory cytokines, such as tumor necrosis factor (TNF)-α, via NF-κB transcription factor [54]. TNF-α is elevated in severe fibrosis patients [2]; therefore, IP-10 expression should be elevated in

response to progression of liver fibrosis.

To clarify why IP-10 expression is not correlated with IL28B SNP, I genotyped IL28B SNP and quantitated the hepatic ISGs. I then analyzed their association, focusing on the progression of liver fibrosis. I found that IP-10 expression is associated with IL28B SNPs only in patients with mild or no fibrosis [36].

Chapter 1

An orally available, small-molecule interferon inhibits viral replication

1-1. Abstract

Most acute HCV infections become chronic and some progress to liver cirrhosis or hepatocellular carcinoma. Standard therapy involves an IFN-α-based regimen, and efficacy of therapy has been significantly improved by the development of protease inhibitors. However, several issues remain concerning the injectable form and the side effects of IFN. Here, I report an orally available, small-molecule type I IFN receptor agonist that directly transduces the IFN signal cascade and stimulates antiviral gene expression. Like type I IFN, the small-molecule compound induces ISG expression for antiviral activity in vitro and in vivo in mice, and the ISG induction mechanism is attributed to a direct interaction between the compound and IFN-α receptor 2, a key molecule of IFN-signaling on the cell surface. My study highlights the importance of an orally active IFN-like agent, both as a therapy for antiviral infections and as a potential IFN substitute.

1-2. Introduction

HCV infection affects 170 million people worldwide [41], and most acute HCV infections become chronic, with some progression to liver cirrhosis or hepatocellular carcinoma. HCV has a plus-strand RNA genome that encodes both structural proteins and the NS proteins 2, 3, 4A, 4B, 5A and 5B. Current standard therapy against chronic HCV infection includes the use of host factor-targeting PEG-IFN-α and RBV [19], which is effective in only 50% of patients chronically infected with HCV genotype 1 [85]. The main causes of this low rate of efficacy may be (i) SNPs in the upstream region of the IL28B gene and (ii) low compliance with the therapy, which must be administered subcutaneously. Regarding the first cause—SNPs—the host factors that are important in the early response to therapy remain unknown. However, recent studies report that genetic variants near IL28B, which encodes IFN-λ3 (interleukin 28B), correlate with the response to treatment of chronic hepatitis C infection using IFN-α/RBV combination therapy [18, 74, 76, 77]. Patients with an rs12979860 SNP genotype of CC are reported to have a stronger response to IFN therapy (up to an 80% SVR rate with the combined therapy) than those with TC or TT genotypes [18]. Regarding the lack of compliance, the current therapy using recombinant IFN is a weekly injectable formulation that is unstable,

requires refrigeration, and is expensive and complex to administer. Furthermore, therapy is often poorly tolerated as a result of the presence of many adverse effects, including flu-like symptoms, hematological abnormalities and adverse neuropsychiatric events, any of which may require early discontinuation [7]. These side effects may result in dose modifications that lead to less-than-optimal responses.

Recent trends in drug development focus on drugs targeted against viral proteins such as NS 3/4A serine protease, RNA helicase, NS4B, NS5A, and NS5B RNA-dependent RNA polymerase [83]. Very recently, two NS3/4A protease inhibitors, telaprevir and boceprevir, have been approved as new anti-HCV agents. Adding such an inhibitor to the standard therapy achieved significantly higher SVR rates, but the issue still remains that using these inhibitors without injectable IFN possibly yields clinical resistance [38]. To overcome this problem and alleviate the low compliance outlined above, an orally available IFN would be valuable because the dosing regimen is less complex.

IFNs induce the expression of a subset of ISG [71], some of which show antiviral activity or are involved in lipid metabolism, apoptosis, protein degradation and inflammation [10]. IFNs are not only effective against HCV infection, but are also essential for innate immunity. Broadly

speaking, type I IFNs (IFN-α and -β) bind to their receptor, causing the phosphorylation and activation of JAK1 and Tyk2, which is followed by the phosphorylation of STATs and subsequent ISG expression. To activate the JAK/STAT pathway, IFN-α requires the IFN-α/β receptor, which consists of 2 subunits, IFNAR1 and IFNAR2. These IFNAR subunits together form a heterodimer upon IFN stimulation. This association of IFNAR2 and IFNAR1 is required to mediate the antiviral, antiproliferative, and apoptotic effects of type I IFNs [53, 58, 80] because the dimerization of IFNARs induces the phosphorylation of the receptor-associated tyrosine kinases, JAK1 and Tyk2, and the phosphorylated JAK kinases then phosphorylate STAT1 and STAT2. In turn, phosphorylated STAT1 and STAT2 bind to IRF9 to form the transcriptional activator ISGF3 that induces the expression of a subset of ISGs [71].

Using quantitative HTS, I identified in this study a novel small molecule that acts like IFN by directly interacting with the type I IFN receptor to drive ISG expression. My results indicate that oral administration of the small-molecule IFN agonist stimulates ISG expression in mice, and that the ISG expression from this small-molecule IFN provides antiviral activity, indicating that the compound may be a potential therapeutic IFN substitute.

1-3. Materials and Methods

Cell culture, mice, and reagents

The #Huh7/3-1 cell line, which expresses HCV replicons, was kindly presented from F. Hoffmann-La Roche (Basel, Switzerland). The cells were cultured in 0.5 mg/mL G418-containing Dulbecco's modified Eagle's medium (DMEM, GIBCO, Grand Island, NY) supplemented with 10% fetal bovine serum (FBS, HyClone, Logan, UT). The replicon construct was derived from pFK-I377neo/NS3-3′/WT, as previously reported [66]. Hc cells (DS Pharma Biomedical, Tokyo, Japan) were cultured in CSC Complete Defined Serum-Free Medium (Cell Systems Corporation, Kirkland, WA) supplemented with SF4ZR-500-D Rocket Fuel. Toll-like receptor (Tlr) knockout (KO) mouse embryonic fibroblasts (MEFs) were purchased from OrientalBioService, Inc. (Kyoto, Japan), Ifnar1 KO MEF was kindly gifted by Prof. Takaoka. 2fTGH, and U1A and U5A cells were kindly gifted by Prof. Stark. Culture conditions for the other cell lines are shown in Table 1. Six-week-old C57BL/6J mice were obtained from Charles River Laboratories (Yokohama, Japan). Chimeric mice harboring a functional human liver cell xenograft were purchased from PhoenixBio (Hiroshima, Japan). The protocol was reviewed by the Institutional Animal Care and Use Committee of Chugai Pharmaceutical Co., Ltd. and all

mouse experiments were performed in accordance with the Guidelines for the Accommodation and Care of Laboratory Animals promulgated in Chugai Pharmaceutical Co., Ltd. Recombinant human IFN-α2a was a kind gift from F. Hoffmann-La Roche. Recombinant murine IFN-αA and human IFN-β1a were purchased from PBL Interferon Source. Recombinant TNF-α and IFN-γ were purchased from R & D Systems (Minneapolis, MN). Imiquimod was purchased from LKT Laboratories (St. Paul, MN). JAK inhibitor I was purchased from Merck (Darmstadt, Germany).

Luciferase assay

Luciferase activity was quantified using the Steady-Glo Luciferase assay system (Promega, Madison, WI) and the EnVision 2013 Multilabel Reader (PerkinElmer, Waltham, MA).

WST-8 assay

The viability of drug-treated Huh-7 cells was determined using a WST-8 cell counting kit (Dojin Laboratories, Tokyo, Japan).

Real-time reverse transcription-polymerase chain reaction (RT-PCR)

Total RNA was extracted using RNeasy (Qiagen, Venlo, Netherlands), and cDNA was synthesized using a Transcriptor First Strand cDNA Synthesis Kit (Roche Applied Science, Indianapolis, IN). Gene expression was measured using the LightCycler 480 System and LightCycler 480 Probes Master (Roche Applied Science). The amplification used 95 °C for 5 min., followed by 50 cycles of: 95 °C for 10 sec., and 60 °C for 30 sec. Human β-actin or rodent glyceraldehyde 3-phosphate dehydrogenase (GAPDH; Applied Biosystems, Foster City, CA) expression was used as the endogenous reference for each sample. Primers and TaqMan probes for genes were designed using the Universal Probe Library Assay Design Center (Roche Applied Science; Table 2). The probes used were from the Roche Universal Probe Library (Roche Applied Science). The samples were run in triplicate for each target gene, and each reference gene was used as an internal control.

Western blotting and immunostaining

Cells were lysed in CelLytic M Cell Lysis Reagent (Sigma-Aldrich St. Louis, MO) containing Protease Inhibitor Cocktail (Sigma-Aldrich,) and PhosSTOP (Roche Applied Science). Rabbit polyclonal antibodies against STAT1, STAT3, STAT6, pY701-STAT1,

pY690-STAT2, pY705-STAT3, pS727-STAT3, pY694-STAT5, pY641-STAT6, pY1022/1023-JAK1, and pY1054/1055-Tyk2 were purchased from Cell Signaling Technology (Danvers, MA). Rabbit polyclonal antibodies against actin, STAT2 and STAT5 were purchased from Santa Cruz Biotechnology (Santa Cruz, CA). Anti-Tyk2 rabbit polyclonal antibody was purchased from Upstate. Anti-IFNAR1 mouse monoclonal (MAB245) and anti-IFNAR2 sheep polyclonal antibodies were purchased from R & D Systems. Anti-NS3, anti-NS5A, and anti-NS5B rabbit polyclonal antibodies were a kind gift from F. Hoffmann-La Roche. Anti-NS4A and anti-NS4B mouse monoclonal antibodies were kindly gifted from the Tokyo Metropolitan Institute of Medical Science. Proteins were detected using the Odyssey Infrared Imaging System (LI-COR, Lincoln, NE). For immunostaining analysis, the cells were fixed on a 35-mm glass-based dish (Iwaki, Tokyo, Japan) with 4% paraformaldehyde, blocked using 5% fetal bovine serum in phosphate-buffered saline, and then incubated with anti-NS3 and anti-NS4A antibodies. The cells were then washed and incubated with Alexa488-labeled anti-rabbit IgG and Alexa568-labeled anti-mouse IgG (Molecular Probes, Eugene, OR) and analyzed using confocal laser microscopy.

JFH-1 antiviral assay

A cured K4 cell line derived from HuH-7 HCV replicon cells was maintained in DMEM supplemented with 10% fetal calf serum (FCS), high-glucose nonessential amino acids, and HEPES (Invitrogen, Carlsbad, CA). The JFH-1/K4 cell line, which was persistently infected with the HCV JFH-1 strain, was maintained under the same conditions as the cured K4 cell line. For the anti-HCV assay of JFH-1/K4 cells persistently infected with the JFH-1 strain, JFH-1/K4 cells were seeded in a 24-well tissue culture plate containing DMEM supplemented with 10% FCS, high-glucose nonessential amino acids, and HEPES (Invitrogen). After overnight incubation, serial dilutions of reagent in growth medium were added. After 72 h, total RNA was purified from the JFH-1/K4 cells using Isogene (Nippon Gene, Tokyo, Japan). HCV-RNA was quantified by real-time PCR as previously reported [75].

Encephalomyocarditis virus (EMCV) cytopathic effect assay

This assay was performed on A549 cells seeded in a 96-well tissue culture plate containing DMEM supplemented with 10% FBS. After overnight incubation, the indicated concentrations of each reagent were added to the growth medium. After 12 h, 100 TCID50/mL EMCV was

added, and after another 48 h, viable cells were stained with 0.5% crystal violet. RNAi experiment using EMCV was also performed on A549 cells seeded in a 96-well tissue culture plate containing DMEM supplemented with 10% FBS. I transfected STAT1- or STAT2-siRNA to A549 cells, and after 72 h, I infected EMCV to the cells and treated them with 1 μM RO8191 or 2 IU/mL IFN. After additional 48 h incubation, I evaluated the cell viability by staining with crystal violet.

GeneChip and data analysis

Total RNA was extracted from 10^7 HCV replicon cells cultured for 8 h in the presence of 2 μM RO8191 or 4 IU/mL IFN-α with TRIzol Reagent (Invitrogen). Reverse transcription, RNA labeling (5 μg of total RNA), hybridization to Human Genome U133 Plus 2.0 Arrays (Affymetrix, Santa Clara, CA), and scanning were performed according to the manufacturer's instructions (Affymetrix, http://www.affymetrix.com). GC-RMA (GeneChip Robust Microarray Analysis) algorithms were used to generate scaled gene expression values. The fold change compared to untreated cells was calculated, and probe sets were selected for genes that were at least 2.0-fold upregulated in RO8191- and IFN-α-treated cells relative to the control cells.

RNA interference

For all double-stranded RNAs, ON-TARGET Plus siRNA reagents (Dharmacon, Lafayette, CA) were used (Table 3). The siRNAs were transiently transfected using Lipofectamine RNAiMAX Transfection reagent (Invitrogen) according to the manufacturer's protocols for reverse transfection.

Plasmids and transfection

IFN-stimulated response element (ISRE) and NF-κB reporter gene were purchased from Clontech (Mountain View, CA). IFNAR2 was cloned into a pCOS2 vector harboring the EF1α promoter. Plasmids were transfected using FuGENE HD (Roche Applied Science) according to the manufacturer's instructions.

Surface plasmon resonance (SPR) measurements

SPR binding studies were performed using a Biacore T100. Recombinant IFNAR2 extracellular domain (ECD) protein was purchased from R & D Systems. The protein (1

mg/mL) was diluted 1:20 with 10 mM sodium acetate buffer (pH 5.0) and mixed with 2 μM RO8191 for stabilization of the binding site. The mixture was immobilized on a Series S sensor chip CM7 using amine coupling. RO8191 and PEG-IFN-α2a (Chugai Pharmaceutical, Tokyo, Japan) were injected onto the sensor chip at a flow rate of 0.03 mL/min. Response curves were generated by subtraction of the background signal generated simultaneously on a control flow cell. Kinetic parameters were obtained by global fitting of the sensorgrams to a 1:1 model using Biacore T100 Evaluation Software, version 2.0.1.

Humanized liver mice study

The chimeric mice were generated by transplanting human primary hepatocytes into severe combined immunodeficient (SCID) mice carrying the urokinase plasminogen activator transgene controlled by an albumin promoter [49]. The chimeric mice used in this study were applied from Inoue *et al.* [29], and had a high substitution rate of human hepatocytes. Six weeks after hepatocyte transplantation, patient serum containing 10^6 copies of HCV genotype 1b was intravenously injected into each mouse. HCV titer reached approximately 10^8 copies/mL and was stable after 4 weeks of HCV injection and persistently infected for 12 weeks. Here, I used

mice after 5 weeks post infection and tested for 2 weeks. The mice were treated for 14 days with RO8191 30 mg/kg/day orally or PEG-IFN-α2a 30 μg/kg subcutaneously twice weekly. HCV RNA in serum was extracted using the acid guanidinium-phenol-chloroform method. Quantification of HCV RNA was performed using real-time RT-PCR based on TaqMan chemistry, as described [75]. HCV inoculations, drug administration, blood collection, and euthanasia were performed under ether anesthesia. Blood samples were taken from the orbital vein and sera were immediately isolated. The protocols for animal experiments were approved by the local ethics committee. The animals received humane care according to NIH guidelines. Patients gave written informed consent before sampling.

Table 1. Culture medium for cell lines.

Cell	Medium	Supplement
HCT116	MaCOY5A	L-Glu, 10 % FBS
Colo201	RPMI	10 % FBS
WiDr	MEM	Non essential amino acid (NEAA), 10 % FBS
T47D	RPMI	HEPES, D-Glu, 0.2 IU/mL bovine insulin, 10 % FBS
MDA-MB-231	Leibovitz's L-15	NaHCO3, 10 % FBS
MDA-MB-435s	Leibovitz's L-15	10 mg/ml insulin, 15 % FBS
KPL4	DMEM (low-Glc)	5 % FBS
PC3	F-12K	10 % FBS
DU145	MEM	NEAA, Sodium pyruvate (SP), 10 % FBS
22Rv1	RPMI	HEPES, D-Glu, SP, 10 % FBS
KYSE-150	49% RPMI, 49% Ham's F12	2 % FBS
Calu-1	MaCOY5A	L-Glu, 10 % FBS
QC56	RPMI	10 % FBS
A549	F-12K	10 % FBS
NCl-H460	RPMI	10 % FBS
Panc-1	DMEM (high-Glc)	10 % FBS
BxPC3	RPMI	HEPES, D-Glu, L-Glu, SP, 10 % FBS
cFPAC	IMDM	10 % FBS
AsPC1	RPMI	15 % FBS
Hs766T	DMEM (high-Glc)	10 % FBS
HT1080	MEM	NEAA, SP, 10 % FBS
2fTGH	MEM	NEAA, SP, 10 % FBS
U1A	MEM	NEAA, SP, 10 % FBS
U5A	MEM	NEAA, SP, 10 % FBS
Vero	MEM	NEAA, SP, 10 % FBS
MEFs	DMEM (high-Glc)	10 % FBS

Table 2. Primer sequences and Universal Probe Library for RT-PCR.

Target	UPL	Forward Primer	Reverse Primer
HCV IRES	75	CATGGCGTTAGTATGAGTGTCG	GGTTCCGCAGACCACTATG
OAS1	37	GGTGGAGTTCGATGTGCTG	AGGTTTATAGCCGCCAGTCA
MxA	79	TTCAGCACCTGATGGCCTA	AAAGGGATGTGGCTGGAGAT
PKR	62	TTTGGACAAAGCTTCCAACC	CGGTATGTATTAAGTTCCTCCATGA
ADAR	39	CGAGAATCCCAAACAAGGAA	CTGGATTCCACAGGGATTGT
BST2	25	CCACCTGCAACCACACTG	CCTGAAGCTTATGGTTTAATGTAGTG
Viperin	39	TGCTTTTGCTTAAGGAAGCTG	TCCCCGGTCTTGAAGAAAT
ICAM-1	71	CCTTCCTCACCGTGTACTGG	AGCGTAGGGTAAGGTTCTTGC
IRF-1	36	GAGCTGGGCCATTCACAC	TTGGCCTTCCACGTCTTG
STAT1	87	CTGCTCCTTTGGTTGAATCC	GCTGAAGTTCGTACCACTGAGA
SOCS1	87	GCCCCTTCTGTAGGATGGTA	CTGCTGTGGAGACTGCATTG
ISG56	9	AGAACGGCTGCCTAATTTACAG	GCTCCAGACTATCCTTGACCTG
RIG-I	69	TGGACCCTACCTACATCCTGA	GGCCCTTGTTGTTTTTCTCA
MDA5	36	AGGCACCATGGGAAGTGAT	ATTTGGTAAGGCCTGAGCTG
LGP2	71	GCCTTGCAAACAGTACAACCT	TCTTCAGCAAGTCCCCAAAC
IFIT3	80	GCAGAGACACAGAGGGCAGT	TGGCATTTCAGCTGTGGA
USP18	75	TCCCGACGTGGAACTCAG	CAGGCACGATGGAATCTCTC
ISG15	76	GCGAACTCATCTTTGCCAGT	AGCATCTTCACCGTCAGGTC
Herc5	53	TGGATTGCTGATGTGGAGAC	CAGGAGATGAAAATATCTCTTGGAT
IP-10	34	GAAAGCAGTTAGCAAGGAAAGGT	GACATATACTCCATGTAGGGAAGTGA
JAK1	47	GAAAATCCAGTTTGCTTCTTGG	CATGGCATTGCAGTCCTCT
JAK2	50	GGTGAAAGTCCCATATTCTGGT	AGGCCACAGAAAACTTGCTC
Tyk2	1	TGGCTTGCTTGAGTTGACAC	ATCCCCAACGGGCTTACT
IFNAR1	65	ATTTACACCATTTCGCAAAGC	CACTATTGCCTTATCTTCAGCTTCT
IFNAR2	22	GCCTCCCCAAAGTCTTGAA	CCCACACTTTCTTCTTTCTGTTG
IRF9	77	AGCCTGGACAGCAACTCAG	AACTGCCCACTCTCCACTTG
STAT2	21	CATACTAGGGACGGGAAGTCG	ATTCTGCAGCATTTCCCACT
murine Oas1b	1	CCTGGTCACGCACTGGTA	CCCATACTCCCAGGCATAGA
murine Pkr	1	CAGAGCCTGCACCTGAAGTA	GCCATTTTTCCTCCCAGTG
murine Mx1	53	TTCAAGGATCACTCATACTTCAGC	GGGAGGTGAGCTCCTCAGT

murine Cxcl10	3	GCTGCCGTCATTTTCTGC	TCTCACTGGCCCGTCATC
murine Ifit3	3	TGAACTGCTCAGCCCACA	TCCCGGTTGACCTCACTC
murine Isg15	71	AGTCGACCCAGTCTCTGACTCT	CCCCAGCATCTTCACCTTTA
murine Mda5	82	CTATTAACCGTGTTCAAAACATGAA	CACCTGCAATTCCAAAATCTTA
murine Rig-i	73	GAAGATTCTGGACCCCACCTA	TGAATGTACTGCACCTCCTCA
murine Socs1	20	GTGGTTGTGGAGGGTGAGAT	CCTGAGAGGTGGGATGAGG
murine Stat1	80	GCAGCACAACATACGGAAAA	TCTGTACGGGATCTTCTTGGA
murine Usp18	13	GCTTGACTCCGTGCTTGAG	CGGGAGTCCACAACTTCACT
murine Tnf	49	TCTTCTCATTCCTGCTTGTGG	GGTCTGGGCCATAGAACTGA
murine Il6	6	GCTACCAAACTGGATATAATCAGGA	CCAGGTAGCTATGGTACTCCAGAA
murine Il10	41	CAGAGCCACATGCTCCTAGA	GTCCAGCTGGTCCTTTGTTT
murine Il12a	49	CCATCAGCAGATCATTCTAGACAA	CGCCATTATGATTCAGAGACTG
murine Il12b	27	GATTCAGACTCCAGGGGACA	TGGTTAGCTTCTGAGGACACATC
murine Ccl2	62	CATCCACGTGTTGGCTCA	GATCATCTTGCTGGTGAATGAGT
murine Ccl3	40	TGCCCTTGCTGTTCTTCTCT	GTGGAATCTTCCGGCTGTAG
murine Ccl4	1	GCCCTCTCTCTCCTCTTGCT	GAGGGTCAGAGCCCATTG

Table 3. siRNA sequences.

siRNA	Dharmacon ID	Sequence
STAT1-1	J-003543-07	5' - CUACGAACAUGACCCUAUC - 3'
STAT1-2	J-003543-09	5' - AGAAAGAGCUUGACAGUAA - 3'
STAT2-1	J-012064-06	5' - GGACUGAGGAUCCAUUAUU - 3'
STAT2-2	J-012064-08	5' - GAUUUGCCCUGUGAUCUGA - 3'
IRF9-1	J-020858-07	5' - CCACCGAAGUUCCAGGUAA - 3'
IRF9-2	J-020858-08	5' - GCGUGGAGCUCUUCAGAAC - 3'
JAK1-1	J-003145-09	5' - CCACAUAGCUGAUCUGAAA - 3'
JAK1-2	J-003145-12	5' - CGGAUGAGGUUCUAUUUCA - 3'
JAK2-1	J-003146-12	5' - UUACAGAGGCCUACUCAUA - 3'
JAK2-2	J-003146-13	5' - AAUCAAACCUUCUAGUCUU - 3'
Tyk2-1	J-003182-09	5' - GCACAAGGACCAACGUGUA - 3'
Tyk2-2	J-003182-10	5' - CAAUCUUGCUGACGUCUUG - 3'
IFNAR1-1	J-020209-05	5' - GCGAAAGUCUUCUUGAGAU - 3'
IFNAR1-2	J-020209-06	5' - UGAAACCACUGACUGUAUA - 3'
IFNAR2-1	J-015411-06	5' - GAGUAAACCAGAAGAUUUG - 3'
IFNAR2-2	J-015411-07	5' - CACCAGAGUUUGAGAUUGU - 3'

1-4. Results

Identification of antiviral small-molecule IFN agonists by high-throughput chemical library screening

HCV replicon cells, which were established ten years ago [45] using a cell line that expresses the HCV genotype 1b subgenomic replicon [66], possess a luciferase gene as a reporter optimized for use in a robust HTS system. The HTS system provides in-depth analysis of primary screening results, including detailed information regarding potency, efficacy and structure-activity relationships. IFNs show strong inhibition using this system and have been used as a positive control in the assay. Many compounds, including HCV protease inhibitors and HCV polymerase nucleoside/non-nucleoside analogs, have been assessed and are being developed for clinical testing. Analysis of data from the combination of target/counterscreen HTS, data from other assays measuring cellular toxicity, *in vitro* sphingolipid biosynthesis and HCV enzymatic activity (including protease and polymerase) allowed me to select compounds with potentially novel modes of action from the primary screen.

A secondary IFN signal assay, using a luciferase reporter gene which was located downstream of the ISRE, eliminated assay-related false-positive compounds. Of the remaining

anti-HCV replicon compounds, one of the most active was an imidazonaphthyridine with the structural formula 8-(1, 3, 4-oxadiazol-2-yl)-2, 4-bis [1, 2-a] [1, 8] (trifluoromethyl) imidazo naphthyridine (RO4948191, hereinafter RO8191) (Fig. 1a). This compound strongly suppressed HCV replicon activity at 72 h in a dose-dependent manner (Fig. 1b, left graph) without inducing host cell toxicity, as measured by the WST-8 (Fig. 1b, right graph) and CellTiter-Glo assays (data not shown). The IC_{50} (50% inhibitory concentration) of the compound in an anti-HCV replicon assay was 200 nM. The compound suppressed viral replication within 24 h and showed even more effective inhibition, without cytotoxicity, after 7 days (Fig. 1c). In addition, the HCV RNA replicon levels significantly decreased after incubation with the compound for 72 h, as determined by real-time RT-PCR analysis (Fig. 2a). Immunostaining showed that levels of the proteins HCV NS3 and NS4A, which are localized mainly in the perinuclear region of the replicon cells, were also reduced after RO8191 treatment for 24 h (Fig. 2b). This treatment also resulted in the disappearance of viral proteins such as NS3, NS4A/B, and NS5A/B, as shown by western blot analysis (Fig. 2c). The luciferase activity of HCV subgenomic genotype 2 replicon cells (JFH1, data not shown) and, surprisingly, the HCV viral titer of JFH1 [82] in a Huh-7/K4 cell line were also reduced by RO8191 treatment (Fig. 2d).

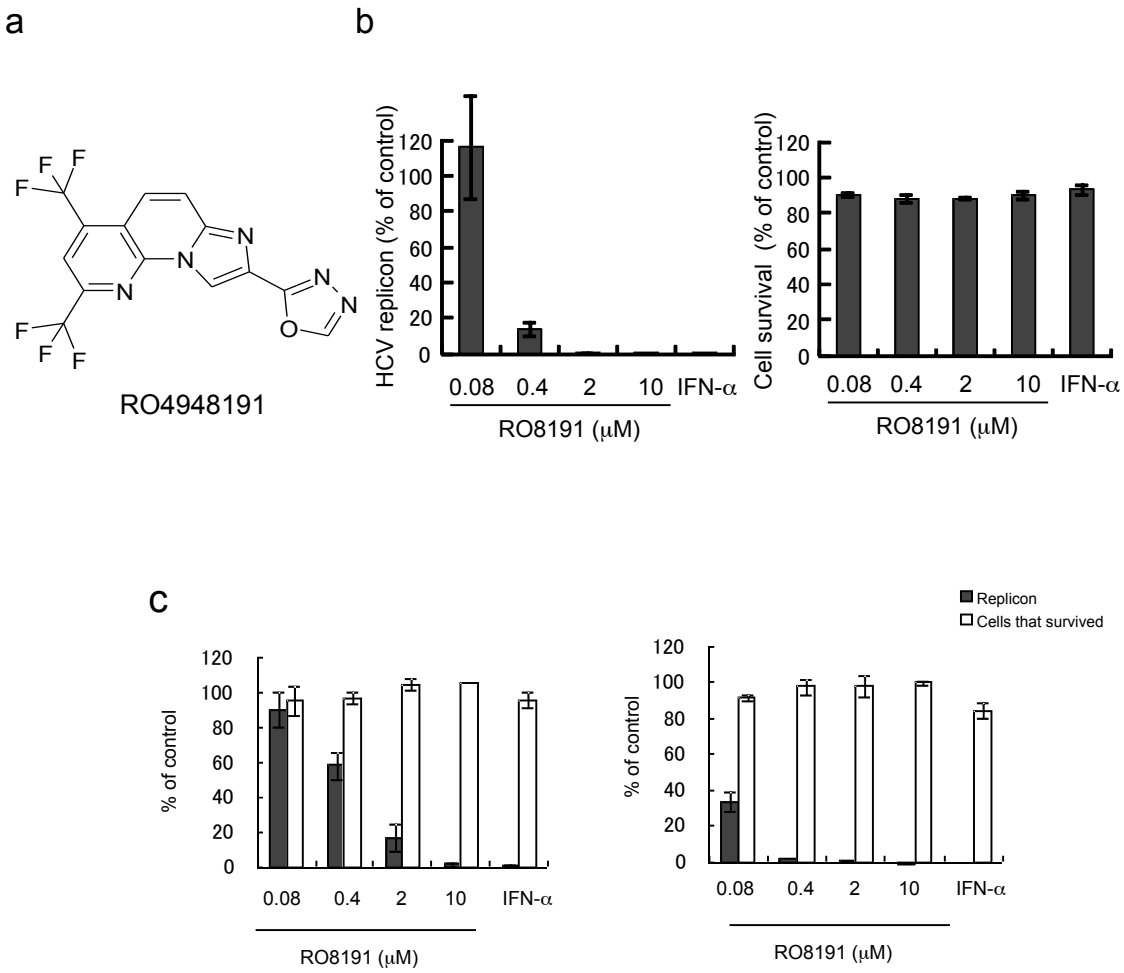

Figure 1. Identification of a small molecule that inhibits HCV replication.

(a) The chemical structure of RO8191. (b) After treatment with various concentrations of RO8191 or 100 IU/mL IFN-α for 72 h, HCV replication levels were examined using a luciferase assay (left graph), and cell viabilities were determined using a WST-8 assay (right graph). The mean values and their SDs were recorded for treated cells as a percentage of the values for untreated cells, and the values represent the means of 3 independent experiments. (c) After treatment with various concentrations of RO8191 for 24 h (left graph) or 7 d (right graph), the replication levels of HCV RNA (genotype 1b) were analyzed using a luciferase assay, and cell viability was determined using a WST-8 assay. The data are mean values, and the bars indicate the standard deviations based on triplicated results.

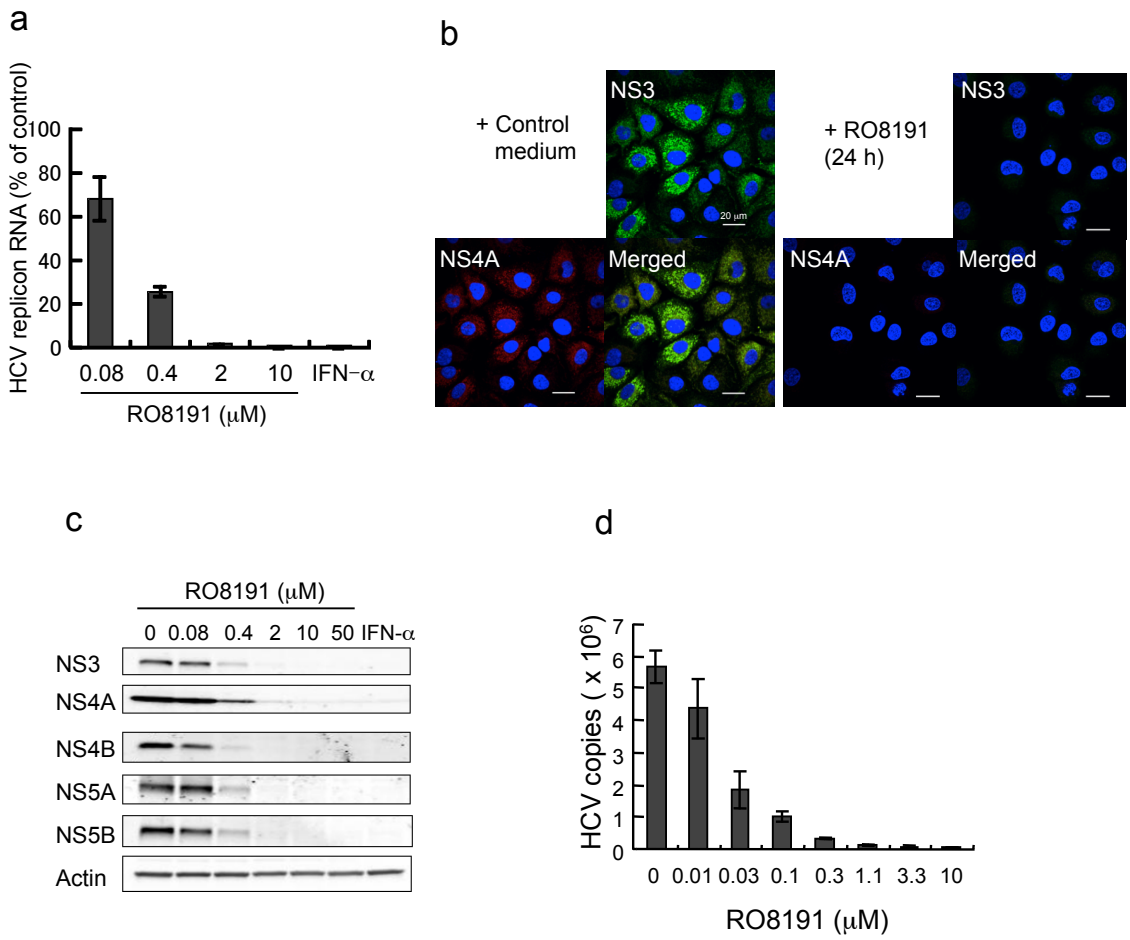

Figure 2. RO8191 inhibits HCV replication.

(a) Total RNA was extracted from HCV replicon cells cultured with the indicated concentration of RO8191 or 100 IU/mL IFN-α for 72 h; HCV RNA levels were analyzed using real-time RT-PCR. The mean values and their SDs were recorded for treated cells relative to the mRNA levels of β-actin, and are shown as a percentage of untreated cells. The values represent the means of 3 independent experiments. (b) HCV replicon cells were treated with control medium (left panels) or 10 μM RO8191 (right panels) for 24 h and immunostained with Hoechst 33452 (blue), anti-NS3 antibody (green), and anti-NS4A antibody (red). The results were then merged (yellow). (c) HCV replicon cells were treated with the indicated concentrations of RO8191 or 100 IU/mL IFN-α for 72 h. Whole cell lysates were immunoblotted with antibodies specific to the indicated HCV NS proteins. (d) After infection with the HCV JFH1 strain, Huh-7/K4 cells were treated with the indicated concentrations of RO8191 for 72 h. Total RNA was extracted, and the HCV RNA levels were analyzed using quantitative real-time RT-PCR.

RO8191 induces IFN signals, ISGs expression and JAK/STAT phosphorylation

To clarify whether RO8191 shows inhibitory activity against another RNA virus, I tested its action in EMCV-infected A549 cells. RO8191 showed a cell-protective activity against EMCV infection similar to that of IFN-α (Fig. 3). Because IFN-α is the most common host cell factor to exert its antiviral activity against HCV [9, 33] by inducing ISG expression [71, 72], I compared the gene expression profiles of IFN-α and RO8191 by conducting a global-scale DNA microarray analysis to identify genes, especially ISGs [11], that were regulated by RO8191. As expected, RO8191 increased the expression of some ISGs (Fig. 4a). The microarray analysis also showed that RO8191 induced the expression of IP-10 (CXCL10), known as an ISG; though in HCV replicon cells, RO8191 did not induce the genes encoding inflammatory cytokines and chemokines (Fig. 4b). And, a reporter gene assay was performed using an NF-κB reporter gene. I transiently transfected the reporter gene to HCV-naïve HuH-7 cells, and then treated them with RO8191 or TNF-α. In Huh-7 cells, NF-κB reporter gene was activated by TNF-α treatment, but not by RO8191 (Fig. 4c). These results suggest that RO8191 induce the IFN-like gene expression specifically.

Real-time RT-PCR analysis also revealed that RO8191 induced many ISGs similar to those

expressed in IFN-α-treated cells (Fig. 5a), suggesting that the antiviral mechanism of RO8191 depends on ISG expression. In addition to HCV replicon cells, I tested the compound in several cancer cell lines and normal human primary hepatocytes (Hc cells). Real-time RT-PCR analysis showed that RO8191 induced ISG expression in cultured cell lines and human primary hepatocytes (Table 4 and Fig. 5b). These results suggest that RO8191 induces an IFN signal, and that the application in clinical of RO8191 is not limited to suppressing HCV infection.

As mentioned earlier, type I IFNs phosphorylate JAK kinases and STAT proteins by inducing a heterodimerization of both IFNAR1 and IFNAR2, and the complexes thus formed transduce signals from IFN. Since RO8191 induces ISGs in a similar profile to IFN-α, I examined the phosphorylation of IFN signaling molecules. Immunoblotting analyses were performed to detect phosphorylated tyrosine (Tyr) and serine (Ser) residues of the STATs and JAK kinases using cells that were treated with 50~5000 times the HCV replicon IC_{50}s of RO8191, IFN-α, IFN-β, and IFN-γ (type II IFN). The degree to which both RO8191 and IFN-β phosphorylated STAT1, STAT5, and STAT6 was similar, as shown in Fig. 6, and the phosphorylation level of STAT2 by RO8191 was quite similar to that of IFN-α. Interestingly, STAT3 and JAK1 were more strongly phosphorylated by RO8191 than by IFN-α, -β, or -γ. On

the other hand, Tyk2 was phosphorylated by type I IFNs, but not by IFN-γ or RO8191, indicating that Tyk2 is dispensable for RO8191 activity (Fig. 6). Taken together, the phosphorylation profile of STAT proteins by RO8191 is generally similar to that of type I IFNs, and the phosphorylation profiles of STAT1–3, 5, 6, and JAK1 in HCV replicon cells treated with RO8191 or type I IFNs suggest a common mechanism that differs from the mechanism in cells treated with type II IFN.

Imiquimod, an IFN inducer and a TLR 7 agonist [24], and other small-molecule ligands recognized by TLRs and RIG-I–like receptors are known to induce ISG expression by inducing IFN [31]. The chemical structure of RO8191 is similar to imiquimod so I examined whether RO8191 has an activity like imiquimod. However, imiquimod did not affect HCV replicon cells (Fig. 7a), nor stimulate STAT1 phosphorylation, whereas RO8191 caused prolonged STAT1 activation (for up to 8 h post-treatment; Fig. 7b). RO8191 is actually a small-molecule and I could not exclude the possibility that the antiviral activity might be induced through TLRs. To confirm that, I tested ISG induction using Tlr3, 4, 7 and 9 KO MEF [23, 24, 27, 84]. I treated the MEFs with RO8191 or murine IFN-αA for 8 h and both induced Oas1b mRNA in wild type and Tlr-KO MEFs (Fig. 7c), demonstrating that RO8191 induces ISG expressions

independently of TLRs. To exclude the possibility that RO8191 acts by inducing type I IFN, I examined its effects in Vero cells that lack the IFN gene locus [12, 51]. Whereas imiquimod did not show IFN-like effects in Vero cells, RO8191 and IFN-α induced the ISRE activation (Fig. 7d), indicating that RO8191 can act without inducing IFN and is quite distinct from imiquimod.

Table 4. RO8191 induces OAS1 expression in various cell lines.

Cancer	Cell line	Fold change ± SD
Colon	HCT116	2333.3 ± 129.2
	Colo201	60.1 ± 6.6
	WiDr	32.2 ± 3.2
Breast	T47D	660.2 ± 12.2
	MDA-MB-231	638.3 ± 33.5
	MDA-MB-435s	34.2 ± 0.6
	KPL4	26.9 ± 4.0
Prostate	PC3	325.3 ± 34.5
	DU145	82.1 ± 1.2
	22Rv1	11.9 ± 1.2
Gastric	KYSE-150	140.1 ± 11.8
Lung	Calu-1	43.2 ± 1.7
	QC56	20.8 ± 2.5
	A549	9.3 ± 1.2
	NCl-H460	3.8 ± 0.2
Pancreas	Panc-1	40.3 ± 7.3
	BxPC3	35.2 ± 1.3
	cFPAC	19.9 ± 2.0
	AsPC1	12.1 ± 4.3
	Hs766T	3.6 ± 0.6
Connective tissue	HT1080	36.2 ± 5.4
Derived from HT1080	2fTGH	21.5 ± 1.2

RO8191 induces OAS1 expression in various cell lines. Total RNA was extracted from various cell lines cultured in the presence of 50 mM RO8191 for 8 h, and OAS1 mRNA levels were then measured using real-time RT-PCR. The mean fold change induction and SD of treated cells compared to untreated cells is based on triplicate determination.

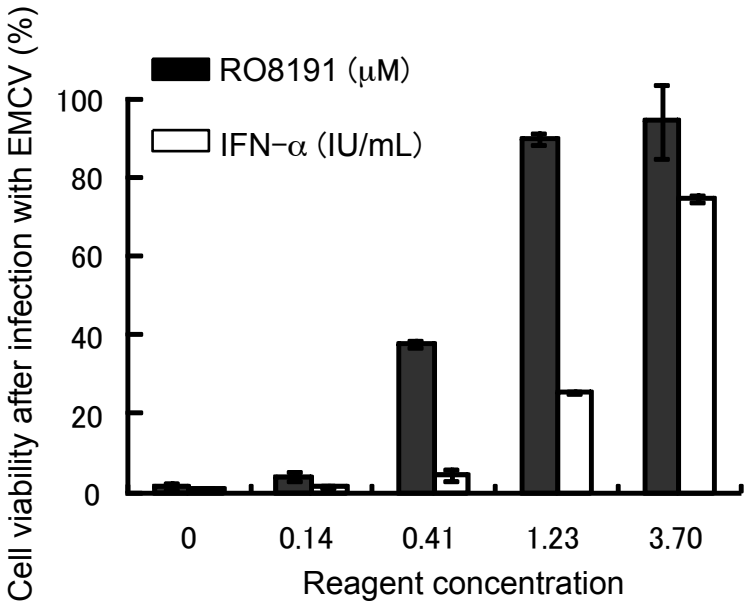

Figure 3. Anti-EMCV effect by RO8191.

The cytopathic effect of EMCV infection was inhibited by the indicated concentrations of RO8191 or IFN-α. Viable cells were stained with crystal violet. The data shown are the mean values and SDs based on experiments performed in quadruplicate.

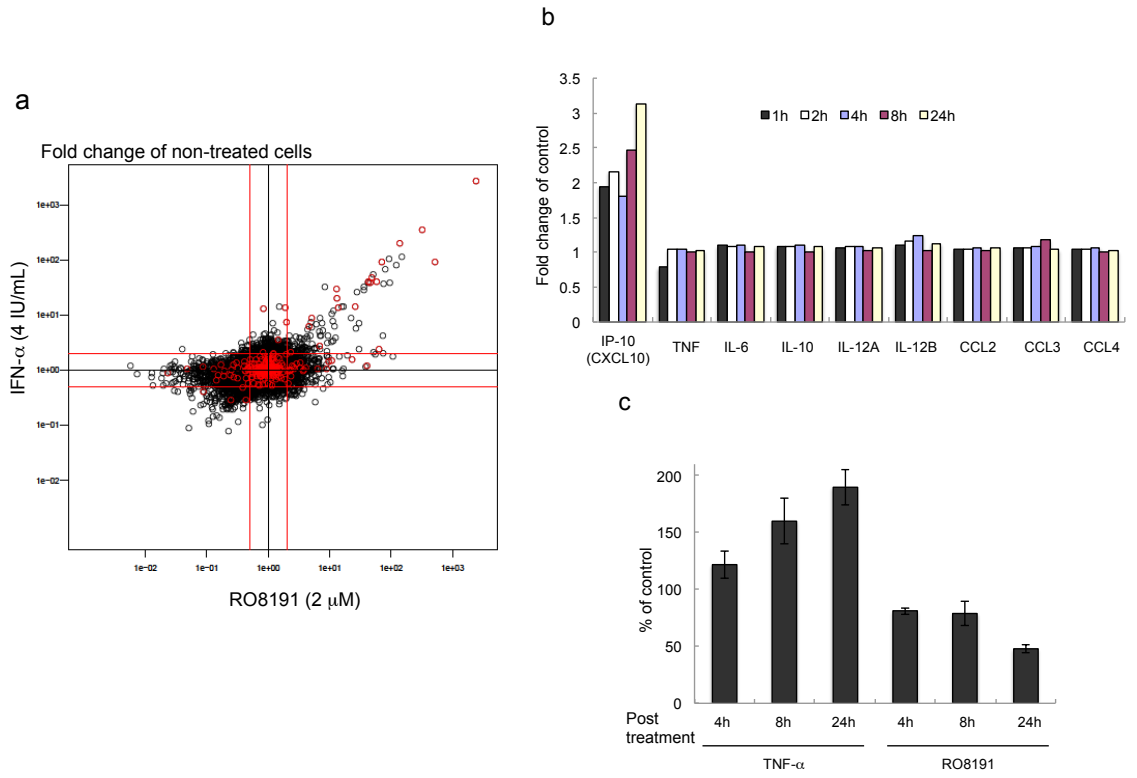

Figure 4. RO8191 induces IFN-like signals.

(a) The fold change in RO8191-treated or IFN-α-treated HCV replicon cells is plotted in comparison to untreated cells. All 54,675 probes (black circles) and 318 ISG probes (red circles) are shown. The red lines to the left and below the center black line indicate 0.5-fold change, and red lines to the right and above the black line indicate 2.0-fold change. (b) Gene expression levels of cytokines and chemokines at indicated time points in the RO8191-treated HCV replicon cells by DNA microarray analysis. (c) NF-κB reporter gene was transiently transfected into the Huh-7 cells, and at 48 h after transfection, the cells were treated with 0.3 ng/mL TNF-α or 50 μM RO8191 and a further 4, 8 or 24 h later, the luciferase activity was measured. The values indicate the mean of fold change.

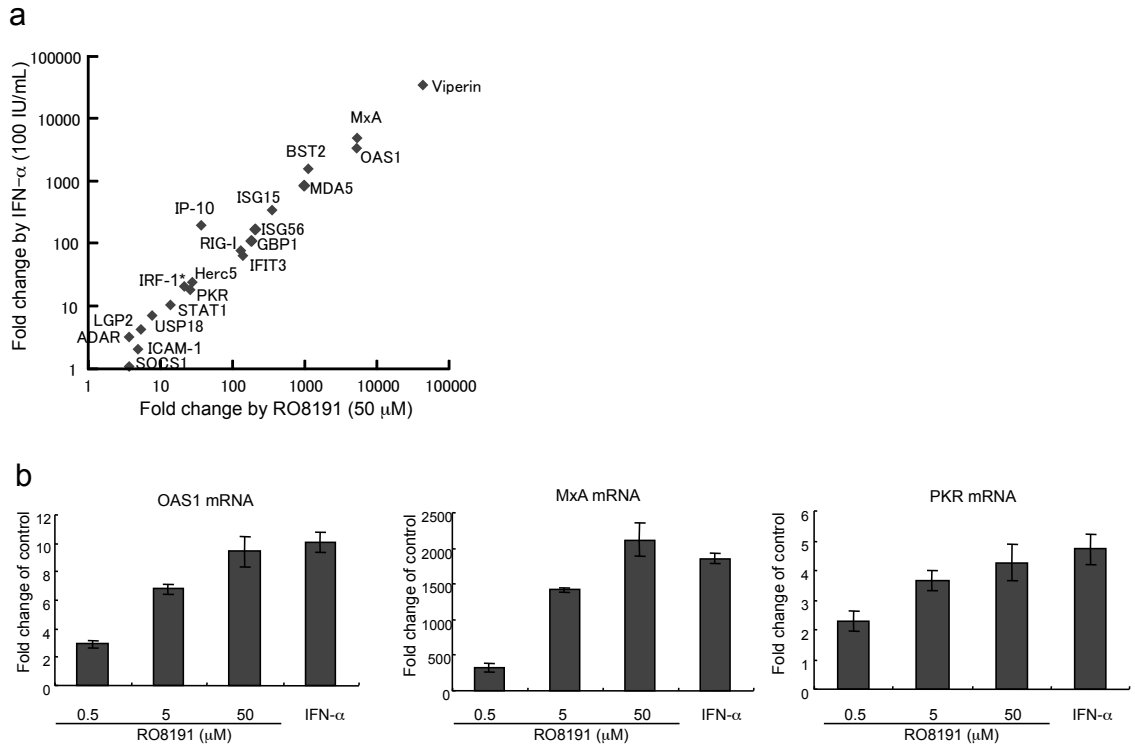

Figure 5. RO8191 induces ISGs expression.

(a) ISG expression levels were measured using real-time RT-PCR. Total RNA was extracted from HCV replicon cells cultured in the presence of 50 μM RO8191 or 100 IU/mL IFN-α for 2 or 8 h and known ISGs were analyzed. Asterisk indicates 2-h treatment with agents. The values shown are the mean fold change induction compared to the mRNA level of human β-actin and the fold change induction compared to untreated cells. (b) ISG expression levels were measured using real-time RT-PCR. The values are listed relative to the mRNA level of human b-actin and represent the mean fold change induction compared to untreated cells. Total RNA was extracted from Hc cells treated with the indicated concentrations of RO8191 or 100 IU/mL IFN-α for 8 h, and the mRNA levels of OAS1, MxA, and PKR (means and SDs) were measured using real-time RT-PCR.

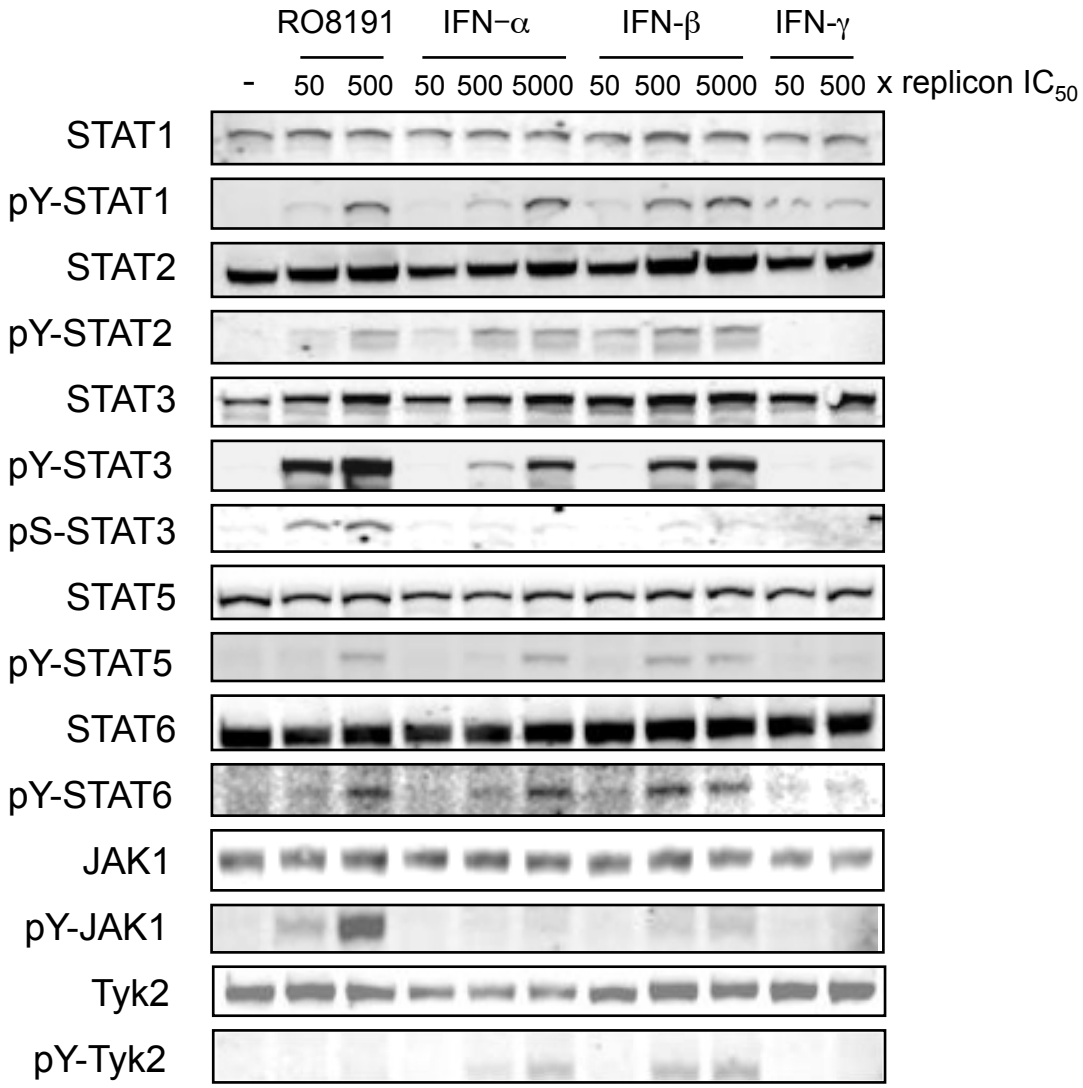

Figure 6. RO8191 activates JAK/STAT pathway.

HCV replicon cells were treated with various concentrations of the indicated agents for 15 min. Total lysates were immunoblotted with antibodies to STATs or JAK kinases. The HCV replicon IC50 of IFN-α was 0.4 IU/mL, that of IFN-β was 3 IU/mL, and that of IFN-γ was 0.3 ng/mL.

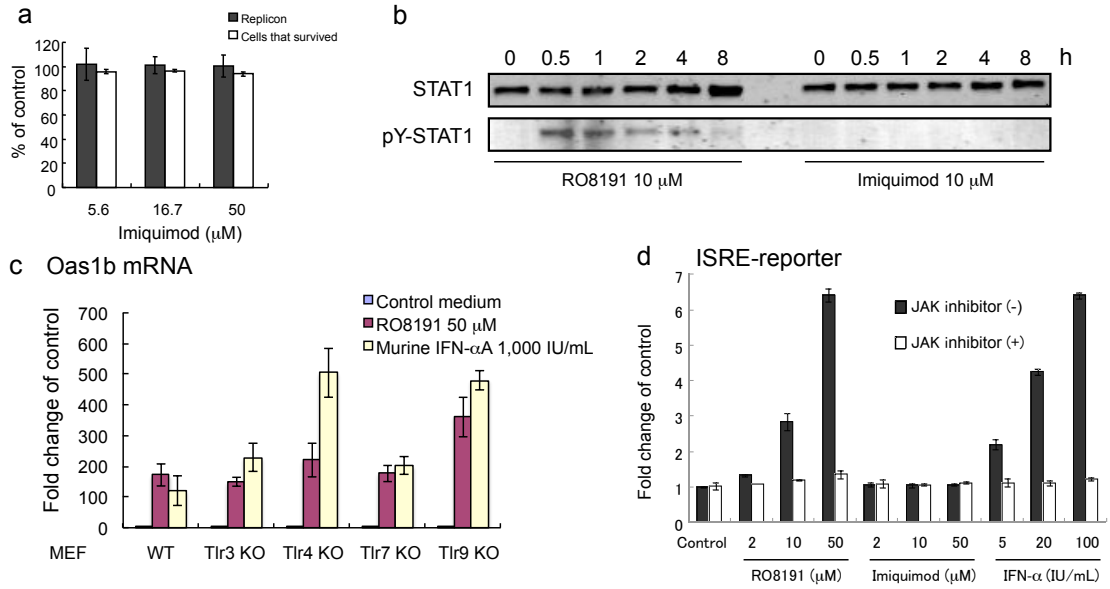

Figure 7. TLR signals cannot induce RO8191-like activity.

(a) After treatment with various concentrations of imiquimod for 72 h, the replication levels of the HCV replicon were analyzed using a luciferase assay, and cell viabilities were determined using a WST-8 assay. (b) Western blot analyses of the phosphorylated and total protein levels of STAT1 in HCV replicon cells cultured in a medium containing 10 μM RO8191 or 10 μM imiquimod at 0.5, 1, 2, 4 and 8 h. (c) Total RNA was extracted from TLR KO MEFs cultured in the presence of 50 μM RO8191 or 1,000 IU/mL murine IFN-αA for 8 h, and the Oas1b mRNA level was analyzed using real-time RT-PCR. The data shown are the mean fold change induction compared to untreated cells, and the bars indicate the standard deviations based on triplicated results. (d) ISRE reporter gene activation by RO8191, imiquimod or IFN-α treatment. ISRE reporter gene was transiently transfected into Vero cells, and 48 h later the cells were treated with RO8191, imiquimod or IFN-α with or without a JAK inhibitor I. After an additional 8 h, luciferase activity was measured.

RO8191 exerts antiviral activity dependent on IFNAR2/JAK1, but is independent of IFNAR1/Tyk2

IFNs require IFN receptor subunits for their activity, and I hypothesized that RO8191 uses the IFN receptor to exert anti-HCV activity. To determine the contributions of IFNAR1 and IFNAR2 toward the anti-HCV replicon activity of RO8191, I suppressed the expression of these receptors using specific siRNA and treated the cells with RO8191 or IFN-α. The knockdown efficiency was determined using RT-PCR in the HCV replicon cells transfected with each siRNA, as shown in Fig. 8. As expected, a knockdown of each receptor subunit decreased the antiviral activity of IFN-α (Fig. 9). IFNAR2 knockdown attenuated the antiviral activity of RO8191 (Fig. 9c and d) but, interestingly, IFNAR1 knockdown did not change the antiviral activity (Fig. 9a and b), suggesting that RO8191 acts independent of IFNAR1. To address whether IFN-α receptor contributes to RO8191 signaling, I evaluated RO8191 using Ifnar1-KO MEF cells [4]. I treated Ifnar1-KO MEFs with 50 μM RO8191 or 1,000 IU/mL of murine IFN-αA for 8 h and analyzed the expression of murine Oas1b mRNA using real-time RT-PCR. Murine IFN induced murine Oas1b mRNA only in wild type MEFs, not in Ifnar1-KO MEFs, although RO8191 induced Oas1b in both wild type and Ifnar1-KO MEFs (Fig. 10). Therefore,

RO8191 induces IFN-like activity even in Ifnar1-KO MEFs.

Since IFNAR2 knockdown reduced RO8191 activity, I focused on and analyzed the IFNAR2 function using RO8191. First, U5A cells, which do not respond to IFN-α because of the lack of IFNAR2 expression [46], were treated with RO8191. Although RO8191 and IFN-α did not induce OAS1 expression in the U5A cells, IFNAR2-overexpressing U5A cells were able to successfully respond to both RO8191 and IFN-α (Fig. 11a and b). RO8191 also induced the OAS1 gene expression in HT1080 and 2fTGH cells, the parental cell lines of U5A cells (Table 4, lowest and second lowest rows). Second, to elucidate whether RO8191 directly interacts with IFNAR2, I obtained a recombinant IFNAR2 ECD protein (N-terminal half of the protein, amino acids from Ile27- Lys243). The protein was subjected to SPR spectroscopy using a Biacore system to directly evaluate the binding activity of the recombinant protein with its possible ligands, RO8191 and IFN-α. The IFNAR2 ECD protein was fixed on the surface of the CM7 sensor chip by amine coupling, and PEG-IFN-α2a and RO8191 were injected as analytes. I comparatively analyzed 0.31 and 0.63 μM of RO8191, and both concentrations showed similar binding affinities of 480.5 and 484.5 nM, respectively (Fig. 11c), whereas a chemically derivatized compound of RO8191 that cannot inhibit HCV replication did not bind to IFNAR2

ECD (data not shown). The SPR results were consistent with 1:1 binding and showed an interaction between RO8191 and the IFNAR2 ECD protein in a dose-dependent manner, indicating that the compound and IFNAR2 may directly interact on the cell surface. In addition to the anti-replicon activity, the phosphorylation of STAT1 by RO8191 was also repressed by IFNAR2 knockdown (Fig. 12a), but the knockdown of IFNAR1 did not inhibit the STAT1 phosphorylation (Fig. 12b), indicating that RO8191 requires IFNAR2 but not IFNAR1 to achieve activity. Similarly, the knockdown of JAK1 attenuated the activity of RO8191 and IFN-α (Fig. 13a and b), while, in contrast, Tyk2 and JAK2 were not required for RO8191 activity (Figs. 13c, d and 14). The phosphorylation of STAT1 by RO8191 was also inhibited by a knockdown of JAK1 (Fig. 15a), but not by a knockdown of Tyk2 (Fig. 15b), indicating JAK1 essentiality for the antiviral activity of RO8191. To confirm Tyk2-independency, I used U1A (Tyk2-deficient) cells and the parental cell, 2fTGH [81], and treated them with 50 μM RO8191 or 100 IU/mL IFN-α for 8 h to analyze the expression of OAS1. As expected from previous reports [43], IFN-α induced the OAS1 expression only in 2fTGH cells but not in U1A cells; however, RO8191 induced the expression in both 2fTGH and U1A cells significantly (Fig. 16). Thus, RO8191 activates ISGs in a JAK1-dependent and Tyk2-independent manner; on the other

hand, IFN-α depends on both factors. Next, I conducted a knockdown of the transcription factors related to type I IFNs activity, STAT1, STAT2 and IRF-9, to clarify whether RO8191 required these factors for antiviral activity. As expected, STAT1-siRNAs partially blocked IFN-γ activity (Fig. 17), which is mediated by STAT1 homodimers [69]. STAT1 was significantly phosphorylated by both RO8191 and IFN-α (Fig. 6); however, the STAT1 knockdown affected neither RO8191 nor IFN-α activity (Fig. 17). I also analyzed the impact of STAT1 knockdown on OAS1 induction by RO8191, and found OAS1 induction by RO8191 was inhibited (Fig. 18). STAT2 and IRF9 knockdown attenuated the inhibitory activity of both RO8191 and IFN-α (Figs. 19 and 20). In summary, RO8191 only binds to IFNAR2 and activates JAK1, STATs, and IRF9, thereby exhibits type I IFN-like activity (Fig. 21).

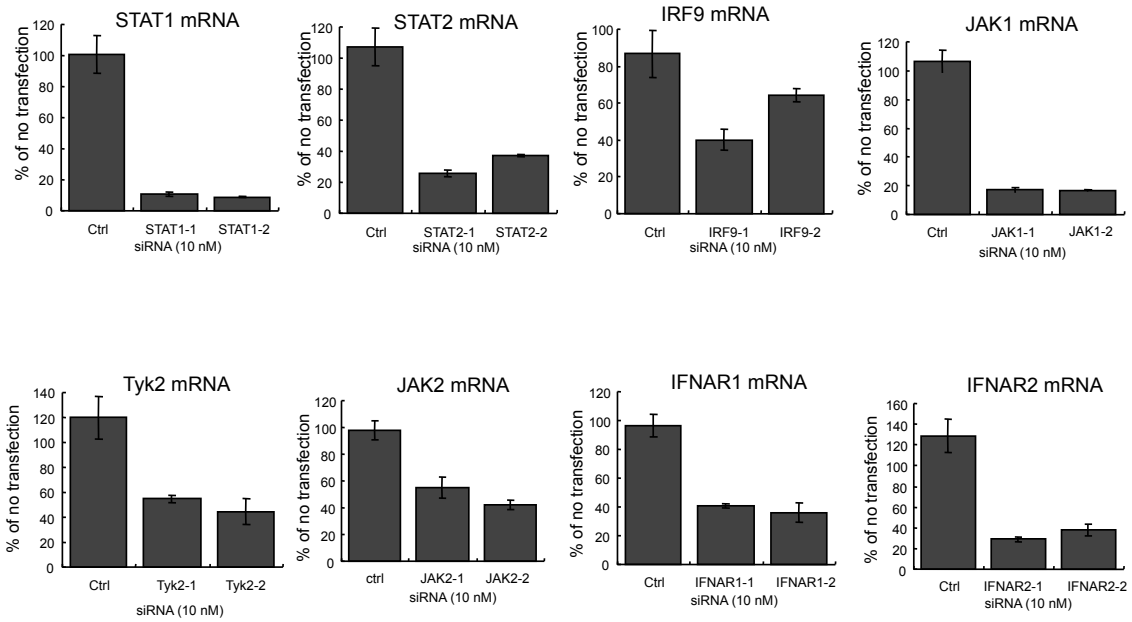

Figure 8. Knockdown efficacy in the HCV replicon cells.

HCV replicon cells transfected with the indicated siRNAs (10 nM). Forty-eight hours after transfection, total RNA was extracted, and the mRNA levels were analyzed using real-time RT-PCR analysis. The data shown are mean values and SDs relative to the mRNA level of human b-actin in non-transfected cells.

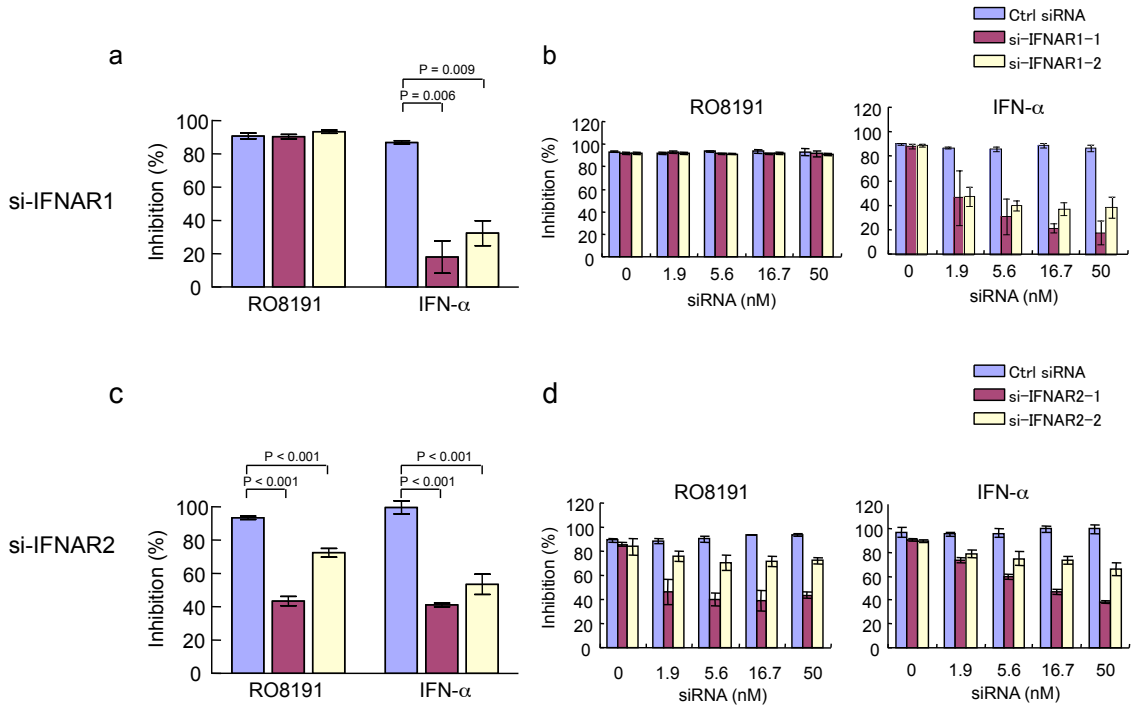

Figure 9. IFNAR2 siRNA inhibits the antiviral activity of RO8191.

(a, c) The anti-HCV replicon activity of RO8191 was attenuated by knockdown of IFNAR2 (c), but not IFNAR1 (a). Inhibition of HCV replicon replication by each agent is shown (the mean and SD from 3 experiments). The HCV replicon cells were transfected with 50 nM of the indicated siRNAs (blue, red, and yellow bars). Forty-eight hours after transfection, the HCV replicon cells were treated with 1.5 μM RO8191 or 3 IU/mL IFN-α for 24 h. Twenty-four hours after treatment with each agent, the replication levels of HCV RNA were analyzed using a luciferase assay. (b, d) Serial dilution includes the data shown in Fig. 9a and c (50 nM siRNA). The inhibition of HCV replicon replication by each agent is shown (the mean and SD from 3 experiments). The HCV replicon cells were transfected with various concentrations of the indicated siRNAs (blue, red, and yellow bars). Twenty-four hours after treatment with each agent, the replication levels of HCV RNA were analyzed using a luciferase assay. Forty-eight hours after transfection, the HCV replicon cells were treated with 1.5 μM RO8191 (left graphs) or 3 IU/mL IFN-α (right graphs) for 24 h. The data were statistically analyzed using Student's t-test.

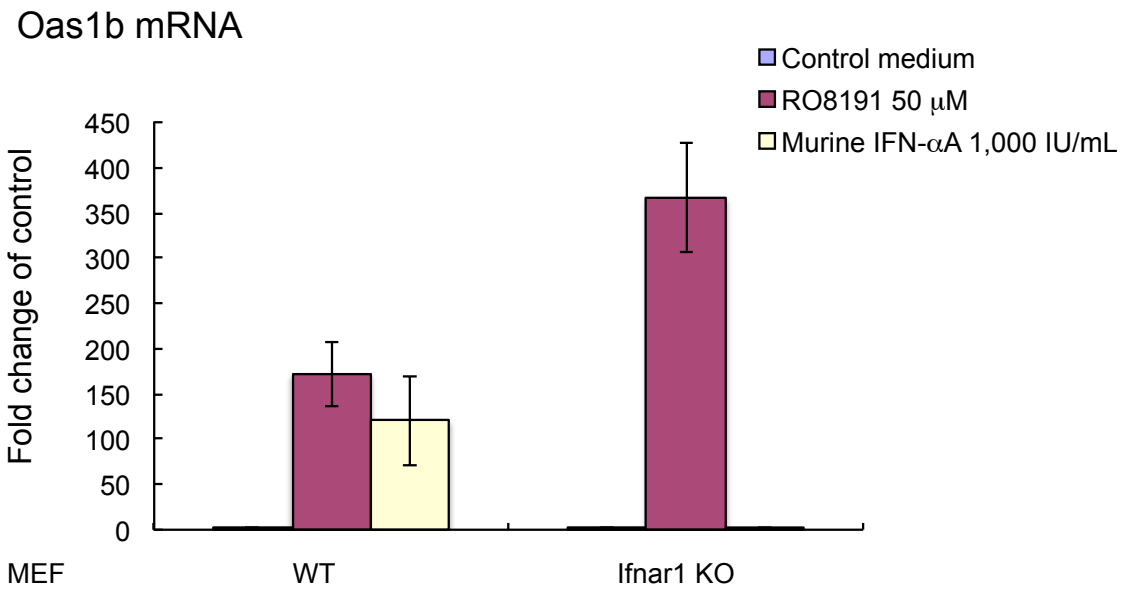

Figure 10. RO8191 induces IFN-like activity in Ifnar1-KO MEFs.

Total RNA was extracted from Ifnar1 KO MEFs cultured in the presence of 50 μM RO8191 or 1,000 IU/mL murine IFN-αA for 8 h, and the Oas1b mRNA level was analyzed using real-time RT-PCR. The data shown are the mean fold change induction compared to untreated cells, and the bars indicate the standard deviations based on triplicated results.

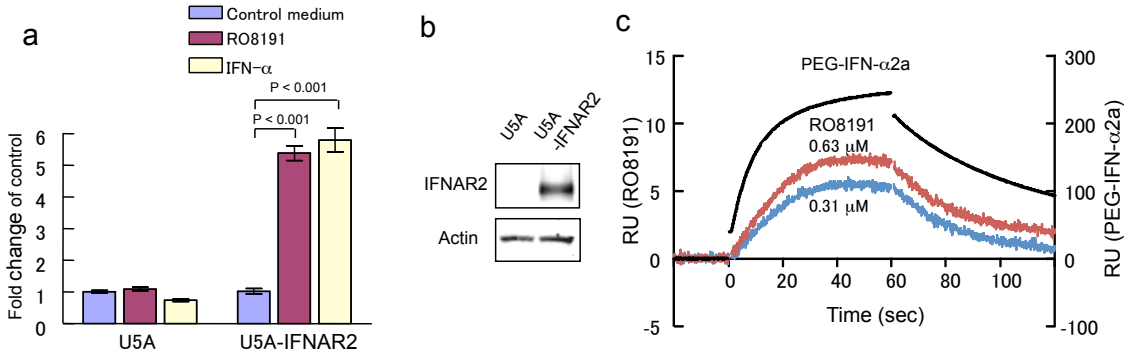

Figure 11. RO8191 requires and binds IFNAR2.

(a, b) U5A cells that lack IFNAR2 were transfected with either an empty vector or a vector expressing the IFNAR2 gene. (a) Forty-eight hours after transfection, the cells were treated with 50 μM RO8191 (red bars) or 100 IU/mL IFN-α (yellow bars). After an additional 8 h of incubation, total RNA was extracted from the U5A cells, and the OAS1 mRNA level was measured using real-time RT-PCR. The values shown are relative to the mRNA level of human β-actin. (b) Forty-eight hours after transfection, the cells were lysed, and the whole cell lysates were immunoblotted with the indicated antibodies. (c) Real-time kinetic SPR analysis of the binding of RO8191 to the IFNAR2 ECD (red and blue lines). The results are consistent with 1:1 binding. PEG-IFN-α2a was also injected as a positive interacting control for IFNAR2 (black line, KD: 30 nM). The data were statistically analyzed using Student's t-test.

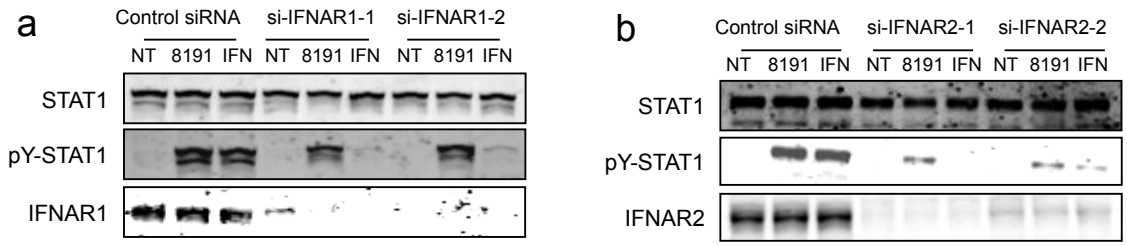

Figure 12. The phosphorylation of STAT1 was attenuated by a knockdown of IFNAR2 (b) but not IFNAR1 (a).

The HCV replicon cells were transfected with the indicated siRNAs (10 nM). Forty-eight hours after transfection, the cells were treated for 15 min with 10 μM RO8191 or 200 IU/mL IFN-α. The total lysates were subjected to western blot analysis to analyze the phosphorylated and total protein levels of STAT1.

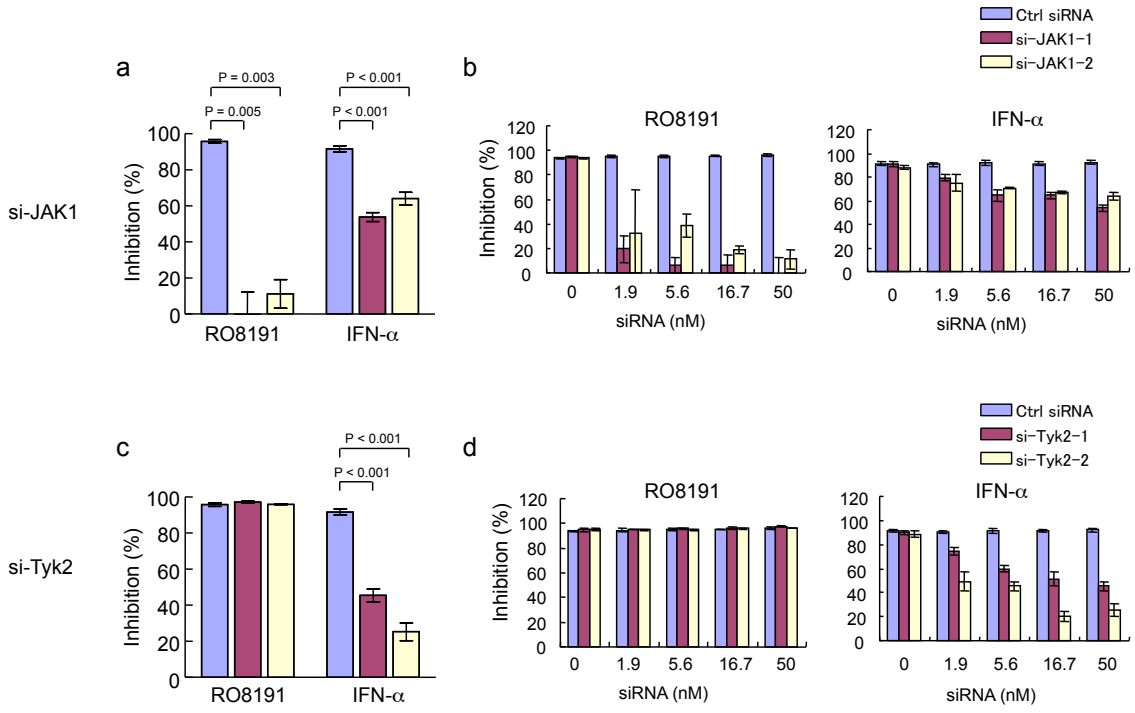

Figure 13. JAK1 siRNA inhibits the antiviral activity of RO8191.

(a, c) The inhibition of HCV replicon replications by each agent is shown (mean and SD). The HCV replicon cells were transfected with 50 nM of the indicated siRNAs (blue, red, and yellow bars). (a, b) The anti-HCV replicon activity of RO8191 was reduced by knockdown of JAK1 (a) but not Tyk2 (b). Forty-eight hours after transfection, the HCV replicon cells were treated with 1.5 μM RO8191 or 3 IU/mL IFN-α. Twenty-four hours after treatment with each agent, the replication levels of HCV RNA were analyzed using a luciferase assay. Serial dilution includes the data shown in Fig. 13a and c (50 nM siRNA). The HCV replicon cells were transfected with various concentrations of the indicated siRNAs (blue, red, and yellow bars). Forty-eight hours after transfection, the HCV replicon cells were treated with 1.5 μM RO8191 (left graphs), 3 IU/mL IFN-α (right graphs). Twenty-four hours after treatment with each agent, the replication levels of HCV RNA were analyzed using a luciferase assay. The data were statistically analyzed using Student's t-test, and differences were considered significant at p values < 0.05.

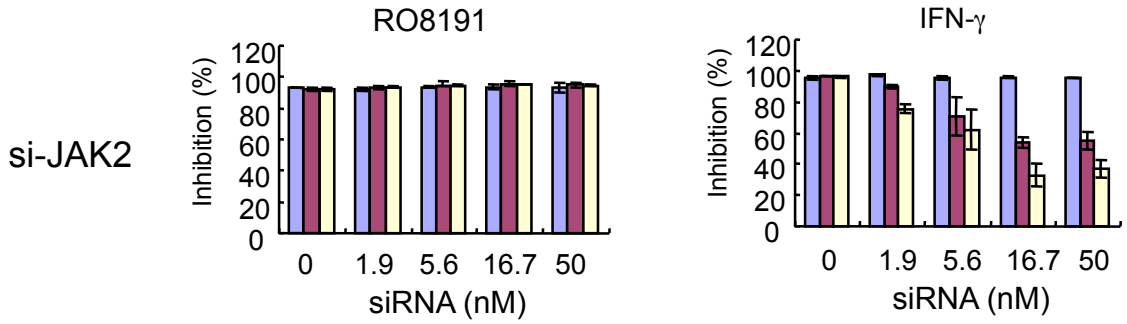

Figure 14. RO8191 induces IFN-like activity in JAK2 siRNA transfected cells.

The anti-HCV replicon activity of RO8191 was not reduced by a knockdown of JAK2. The inhibition of HCV replicon replications by each agent is shown (means and SDs). The HCV replicon cells were transfected with various concentrations of the JAK2 siRNAs (blue, red, and yellow bars). Forty-eight hours after transfection, the HCV replicon cells were treated with 1.5 μM RO8191 (upper graph) or 50 ng/mL IFN-γ (lower graph). Twenty-four hours after treatment with each agent, the replication levels of HCV RNA were analyzed using a luciferase assay.

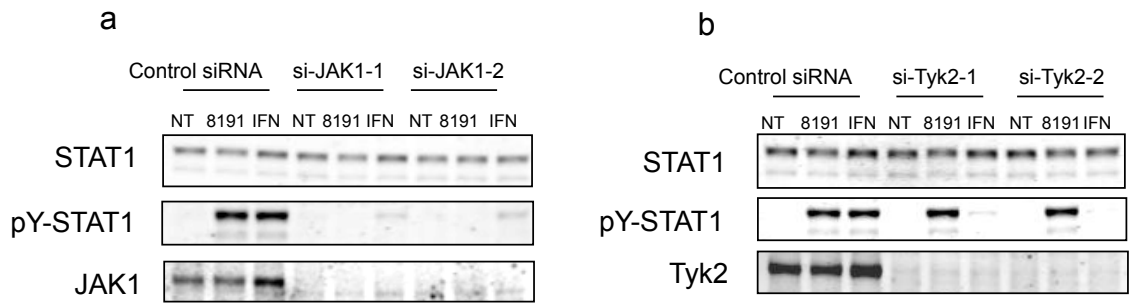

Figure 15. The phosphorylation of STAT1 was attenuated by knockdown of JAK1 (a) but not Tyk2 (b).

The HCV replicon cells were transfected with the indicated siRNAs (10 nM). Forty-eight hours after transfection, the cells were treated for 15 min with 10 μM RO8191 or 200 IU/mL IFN-α. Total lysates were subjected to western blot analysis in order to analyze the phosphorylated and total protein levels of STAT1.

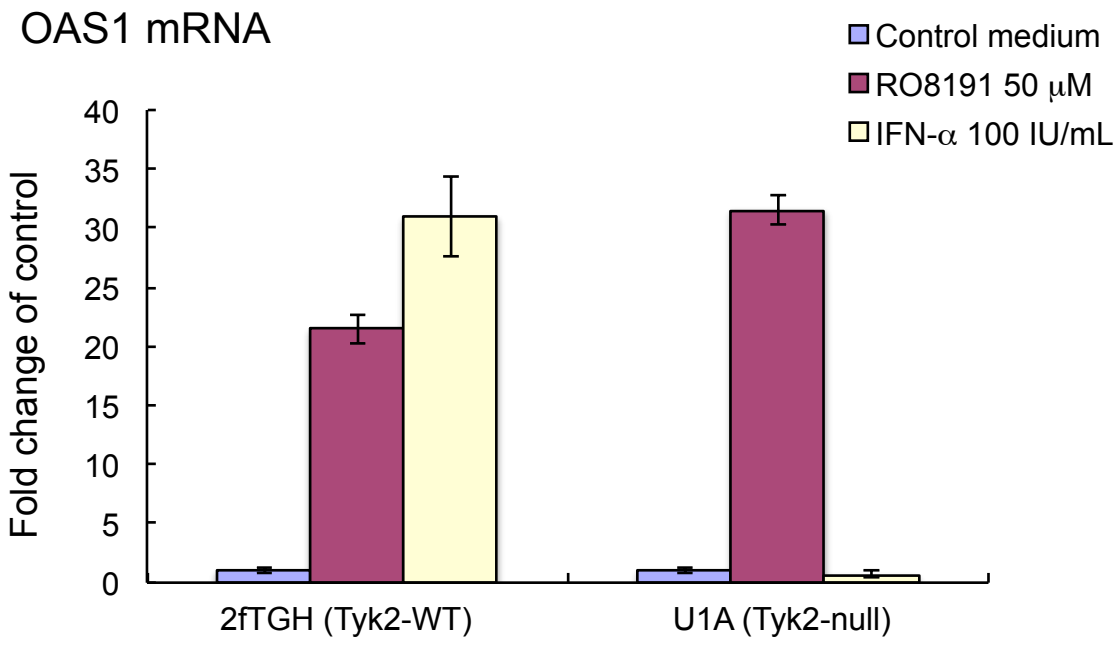

Figure 16. RO8191 induces IFN-like activity in Tyk2-deficient cells.

Total RNA was extracted from 2fTGH and U1A cells cultured in the presence of 50 μM RO8191 or 100 IU/mL IFN-α for 8 h, and the OAS1 mRNA level was analyzed using real-time RT-PCR. The data shown are the mean fold change induction compared to untreated cells, and the bars indicate the standard deviations based on triplicated results.

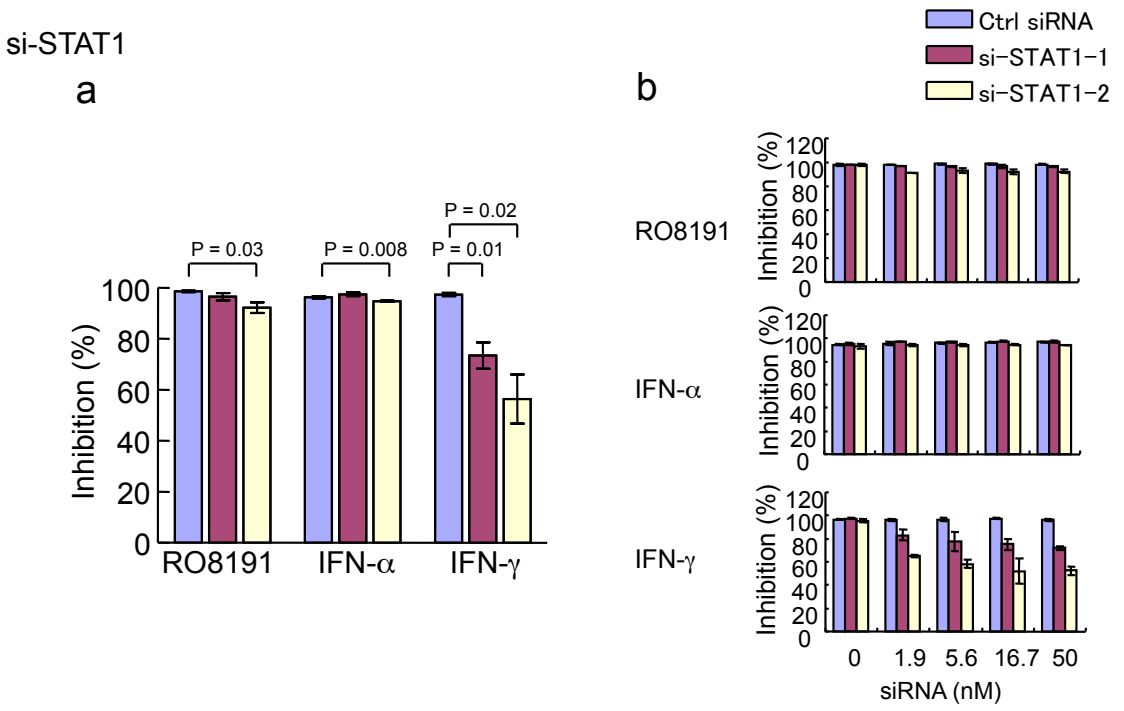

Figure 17. RO8191 activity in STAT1 siRNA transfected cells.

The inhibition of HCV replicon replications by each agent is shown (mean and SD). The HCV replicon cells were transfected with 50 nM of the STAT1 siRNAs (blue, red, and yellow bars). (a) Forty-eight hours after transfection, the HCV replicon cells were treated with 1.5 μM RO8191, 3 IU/mL IFN-α, or 50 ng/mL IFN-γ. Twenty-four hours after treatment, the replication levels of HCV RNA were analyzed using a luciferase assay. (b) Serial dilution includes the data shown in Fig. 17a (50 nM siRNA). The HCV replicon cells were transfected with various concentrations of the indicated siRNAs (blue, red, and yellow bars). Forty-eight hours after transfection, the HCV replicon cells were treated with 1.5 μM RO8191 (top graph), 3 IU/mL IFN-α (middle graph) or 50 ng/mL IFN-γ (bottom graph). Twenty-four hours after treatment, the replication levels of HCV RNA were analyzed using a luciferase assay. The data were statistically analyzed using Student's t-test, and differences were considered significant at p values < 0.05.

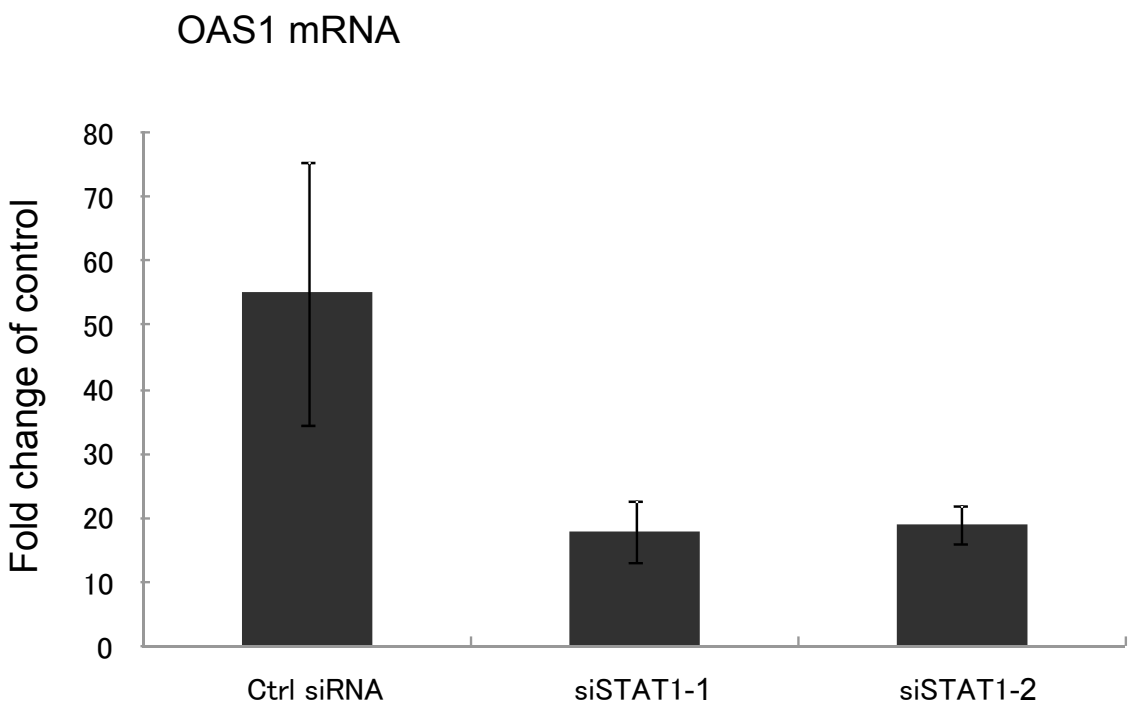

Figure 18. OAS1 induction by RO8191 in STAT1 siRNA transfected cells.

Sixty-four hours after indicated 10 nM siRNA transfection, I treated the cells with 10 μM RO8191 for 8h. Then, RNA was extracted from the cells and OAS1 expression was determined by RT-PCR. The data are mean values, and the bars indicate the standard deviations.

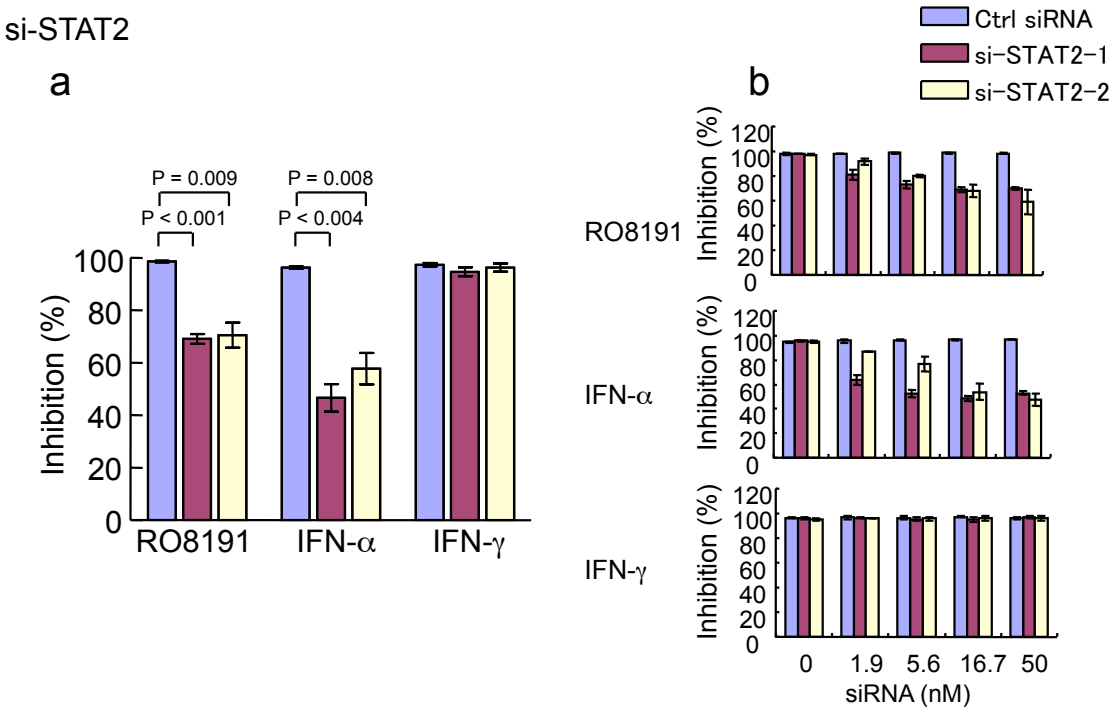

Figure 19. RO8191 activity in STAT2 siRNA transfected cells.

The inhibition of HCV replicon replications by each agent is shown (mean and SD). The HCV replicon cells were transfected with 50 nM of the STAT2 siRNAs (blue, red, and yellow bars). (a) Forty-eight hours after transfection, the HCV replicon cells were treated with 1.5 μM RO8191, 3 IU/mL IFN-α, or 50 ng/mL IFN-γ. Twenty-four hours after treatment, the replication levels of HCV RNA were analyzed using a luciferase assay. (b) Serial dilution includes the data shown in Fig. 19a (50 nM siRNA). The HCV replicon cells were transfected with various concentrations of the indicated siRNAs (blue, red, and yellow bars). Forty-eight hours after transfection, the HCV replicon cells were treated with 1.5 μM RO8191 (top graph), 3 IU/mL IFN-α (middle graph) or 50 ng/mL IFN-γ (bottom graph). Twenty-four hours after treatment, the replication levels of HCV RNA were analyzed using a luciferase assay. The data were statistically analyzed using Student's t-test, and differences were considered significant at p values < 0.05.

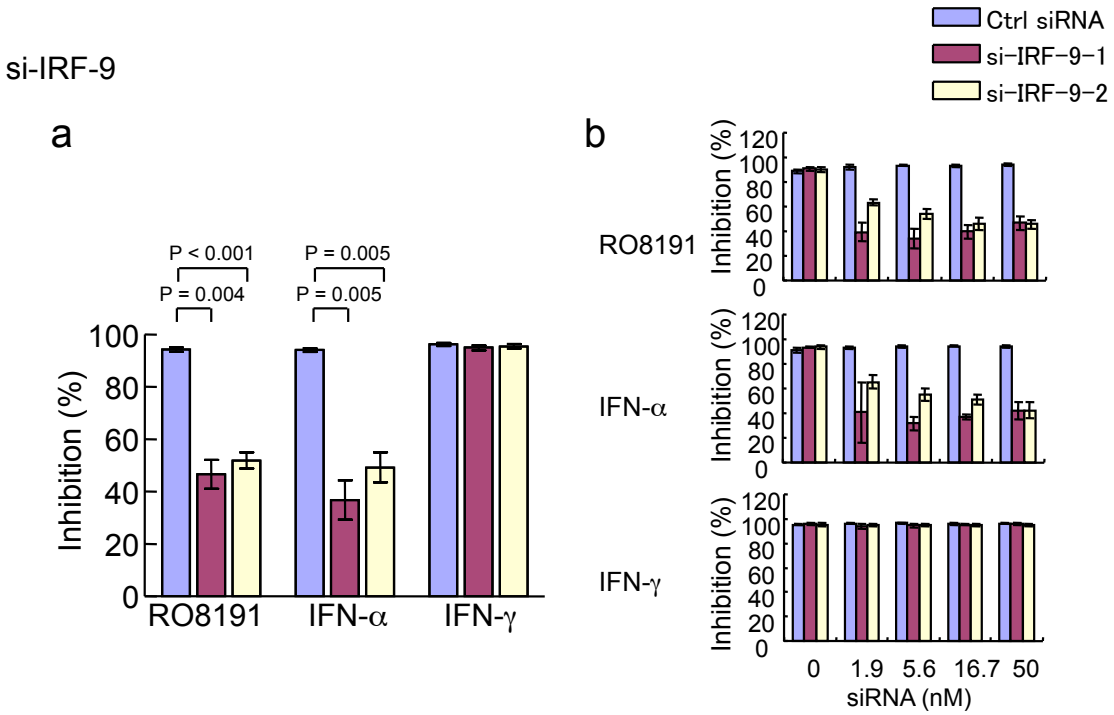

Figure 20. RO8191 activity in IRF-9 siRNA transfected cells.

The inhibition of HCV replicon replications by each agent is shown (mean and SD). The HCV replicon cells were transfected with 50 nM of the IRF-9 siRNAs (blue, red, and yellow bars). (a) Forty-eight hours after transfection, the HCV replicon cells were treated with 1.5 μM RO8191, 3 IU/mL IFN-α, or 50 ng/mL IFN-γ. Twenty-four hours after treatment, the replication levels of HCV RNA were analyzed using a luciferase assay. (b) Serial dilution includes the data shown in Fig. 19a (50 nM siRNA). The HCV replicon cells were transfected with various concentrations of the indicated siRNAs (blue, red, and yellow bars). Forty-eight hours after transfection, the HCV replicon cells were treated with 1.5 μM RO8191 (top graph), 3 IU/mL IFN-α (middle graph) or 50 ng/mL IFN-γ (bottom graph). Twenty-four hours after treatment, the replication levels of HCV RNA were analyzed using a luciferase assay. The data were statistically analyzed using Student's t-test, and differences were considered significant at p values < 0.05.

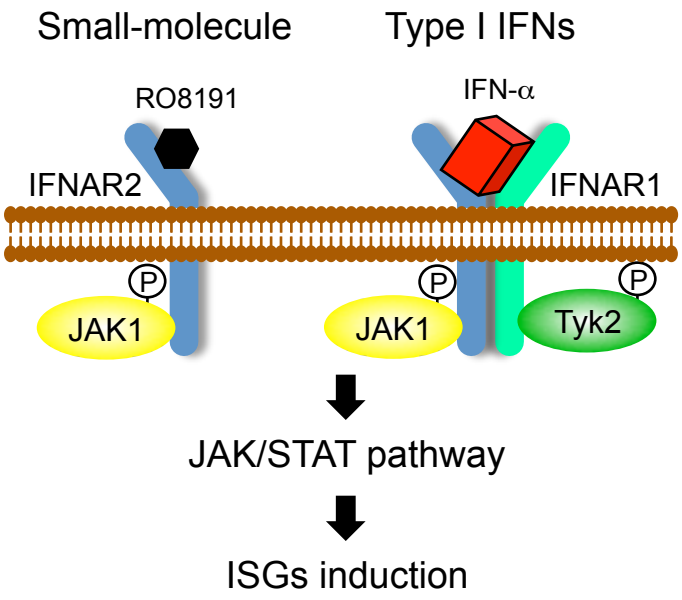

Figure 21. A model showing the pathways of RO8191 and IFN-α.

RO8191 binds to IFNAR2 and activates JAK1, STATs, and IRF9, thereby exhibiting type I IFN-like activity.

RO8191, an IFNAR2 agonist, stimulates IFN signals in mice

To evaluate whether RO8191 could be a clinical lead for drug development, I studied the effects of RO8191 on IFN signaling in mice. The compound or vehicle was orally administered to mice and, 24 h after treatment, the liver was removed and examined. The antiviral genes Oas1b, Mx1, and Pkr were significantly induced in the livers of mice treated with RO8191 (Table 5). As expected, gene homologs that were induced in the livers of HCV patients treated with PEG-IFN-α2b [67] were also induced in mouse liver (Ifit3, Isg15, Mda5, Rig-I, Socs1 and Stat1; Table 5). In addition, genes that had previously been reported to be induced by IFN-β in mouse liver [14] were also induced in the livers of RO8191-treated mice (Cxcl10, Ifit3, Isg15, Socs1 and Usp18; Table 5). I also measured inflammatory cytokine and chemokine expressions, and RO8191 did not significantly induce the expression of these genes (Table 6). To evaluate anti-HCV activity of RO8191 *in vivo*, RO8191 was orally administered to HCV-infected humanized liver mice [49]. The results of this humanized liver mice study showed that RO8191 reduced HCV titer *in vivo* (Fig. 22). These data show that RO8191 stimulates IFN signaling and is an orally available agent in mice.

Table 5. ISG expression in the livers of RO8191 treated mice.

Gene	Entrez ID	Fold change ± SD			p-value
murine Oas1	NM_001083925	3.0	±	0.72	0.003
murine Mx1	NM_010846	2.1	±	0.15	0.0003
murine Pkr	NM_011163	1.4	±	0.21	0.009
murine Cxcl10	NM_021274	1.7	±	0.63	0.097
murine Ifit3	NM_010501	2.5	±	0.48	0.001
murine Isg15	NM_015783	2.3	±	0.41	0.002
murine Mda5	NM_027835	1.6	±	0.22	0.003
murine Rig-i	NM_172689	2.1	±	0.16	0.00003
murine Socs1	NM_009896	2.6	±	1.04	0.057
murine Stat1	NM_009283	1.8	±	0.21	0.001
murine Usp18	NM_011909	2.6	±	0.69	0.017

ISG expression levels were measured using real-time RT-PCR. Values are listed relative to the mRNA levels of rodent Gapdh and represent the mean fold change induction compared to vehicle-administered mice. Twenty-four hours after oral administration of 30 mg/kg RO8191 or vehicle (including 10% dimethyl sulfoxide and 10% Cremophor) to mice, total RNA was extracted from the mouse livers, and the mRNA levels of murine ISGs were measured using real-time RT-PCR. The data shown are the means and SDs of 4 mice per group. The data were statistically analyzed using Student's t-test, and differences were considered significant at p values < 0.05.

Table 6. Cytokine and chemokine gene expression in the livers of RO8191-treated mice.

Gene	Fold change ± SD	p-value
Tnf	2.93 ± 2.37	0.20131
Il6	1.35 ± 1.74	0.81617
Il10	2.53 ± 0.80	0.07623
Il12a	Undetectable	
Il12b	1.07 ± 0.09	0.76622
Ccl2	2.63 ± 1.70	0.13037
Ccl3	1.36 ± 0.90	0.58189
Ccl4	3.08 ± 2.52	0.16316

Gene expressions of cytokines and chemokines were determined by real-time RT-PCR analysis. Samples are the same ones that were used for Table 5. Values are listed relative to the mRNA levels of rodent Gapdh and represent the mean fold change induction compared to vehicle-administered mice. The data shown are the means and SDs of 4 mice per group. The data were statistically analyzed using Student's t-test, and differences were considered significant at p values < 0.05.

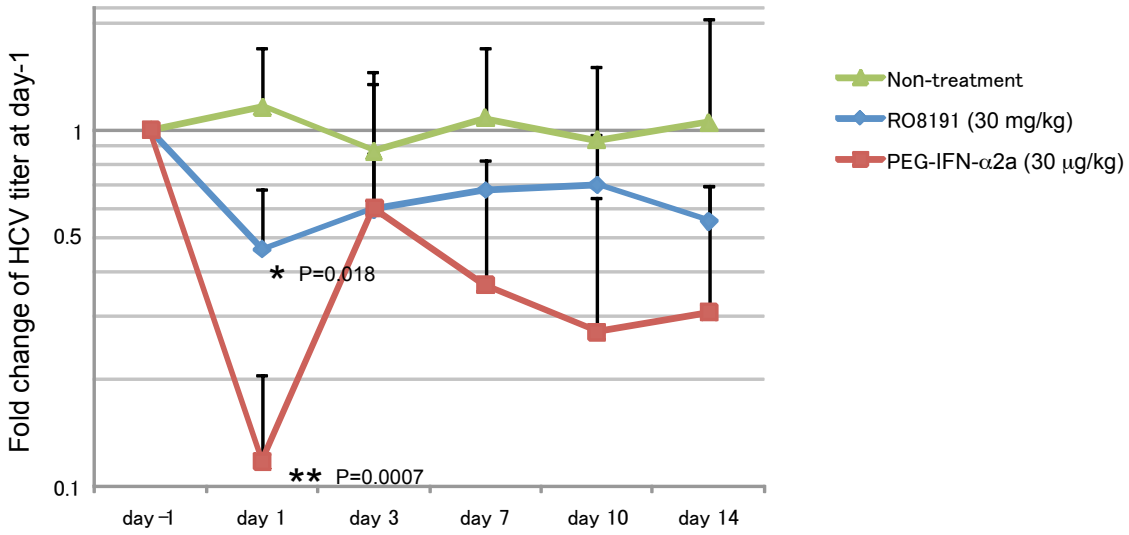

Figure 22. RO8191 reduced HCV titer *in vivo*.

The mice were treated for 14 days with RO8191 30 mg/kg/day orally or PEG-IFN-α2a 30 μg/kg subcutaneously twice weekly. Time course of serum HCV RNA levels in mice treated with RO8191 (red line, n=5), PEG-IFN-α2a (blue line, n=4) or no treatment (green line, n=8) is shown. The data are mean values, and the bars indicate the standard deviations.

1-5. Discussion

In this study, I identified a small-molecule IFN receptor agonist, RO8191, by quantitative HTS of a chemical library. This compound showed antiviral activity against both HCV and EMCV, suggesting a broad spectrum of target viruses. To learn more about the possible mechanism of action of IFN signal induction by RO8191, I investigated IFN-induced signaling and ISG induction by the small-molecule compound *in vitro* and *in vivo*. A comparison of microarray expression profiles in HCV replicon cells stimulated by IFN-α or RO8191 indicates that the IFN signal was induced not only by IFNs, but also by the small-molecule compound (Figs. 4a and 5a). Thus, this compound is an IFN-α-like small molecule, but the mechanism of the RO8191 antiviral activity remained unknown. Therefore, I examined the JAK/STAT activation pathway, which includes key players in the IFN signaling cascade.

Like type I IFNs, RO8191 significantly phosphorylates and activates STATs, in particular, STAT1 and STAT2 (Fig. 6). Intriguingly, in HCV replicon cells, STAT1 expression knockdown did not affect the antiviral activity of RO8191 or IFN-α, although IFN-γ activity was inhibited (Fig. 17). These data suggest that, in addition to inducing similar gene expression, RO8191 and IFN-α exhibit similar STAT phosphorylation profiles. Although RO8191- and

IFN-α-mediated antiviral activity remained constant when STAT1 expression was reduced, this could be because IFN-α signaling in HuH-7 cells requires minimal amounts of STAT1 protein and STAT1 expression was not reduced below such a critical threshold by siRNA in my system. In contrast, the inhibitory activity of RO8191 was attenuated to the same extent as that of IFN-α when the expression of other components of ISGF3 (STAT2 and IRF-9) were reduced by siRNA (Figs. 19 and 20). Incidentally, STAT1 siRNA did not attenuate RO8191 or IFN activity in EMCV-infected A549 cells (Fig. 23), which supports the notion that STAT2 is an essential component of type I IFN signaling [42]. Type I IFN stimulates the formation of other STAT-containing complexes, including STAT1:STAT1, STAT3:STAT3 and STAT5:STAT5 homodimers, as well as STAT1:STAT3 and STAT2:STAT6 heterodimers [20, 21, 44]. Like IFN, RO8191 induced the phosphorylation of STAT1 and STAT2, which function as a gateway to the type I IFN signal cascade, and stimulated the phosphorylation of STAT3, 5 and 6. Another possible cause for the fact that STAT1 knockdown did not show any effect on RO8191 inhibition could be compensation by these IFN signaling-stimulated STAT complexes. This finding matches the recent report by Perry *et al.* on the STAT dependency of IFN activity against Dengue virus, that belongs to flavivirus [57]. They showed that STAT2 mediates IFN

antiviral signals even in STAT1 KO cells and they discussed the possibility that other STAT family proteins would compensate for STAT1 deficiency. In summary, with regards to the activation of transcription factors and ISG expression, RO8191 and IFN-α mediate the same pathway.

IFNs activate JAK kinases via IFN receptors to induce STAT phosphorylation. RO8191 robustly phosphorylated JAK1 (Fig. 6) in comparison with IFN-α or -β and therefore I focused on IFNAR2 (a JAK1-binding subunit of the type I IFN receptor). As with IFN-α, the activity of RO8191 was inhibited by IFNAR2 knockdown (Fig. 9c). The suggestion that IFNAR2 is an essential molecule for RO8191-induced signal transduction is supported by the fact that an IFNAR2-deficient cell line, U5A, did not respond to RO8191. Furthermore, after IFNAR2 expression had been complemented in the U5A cells, ISG induction by both RO8191 and IFN-α recovered (Fig. 11a and b). The mechanism was directly explained by SPR spectroscopy, which showed an interaction between RO8191 and the IFNAR2 ECD (Fig. 11c). RO8191 strikingly phosphorylates the IFNAR2-associated kinase JAK1, when compared to other IFN-treated cell lysates (Fig. 6). JAK1 siRNA expression inhibited RO8191 activity (Fig. 13a), indicating that JAK1 is also an essential molecule for RO8191 activity. Interestingly, RO8191 activity remains

static when IFNAR1 expression is knocked down, unlike IFN-α activity (Fig. 9a). The IFNAR1-binding-kinase Tyk2 is not required for RO8191 activity (Fig. 13b) and Tyk2 was not phosphorylated (Fig. 6) by RO8191. Also, RO8191 induced its signal even in the Ifnar1 KO MEF and the Tyk2-deficient cell line (Figs. 10 and 16). IFN-α induces a signal via IFNAR1/Tyk2 and IFNAR2/JAK1, although RO8191 and IFN-α induce common ISGs, RO8191 activity was dependent only on IFNAR2/JAK1.

I therefore propose a novel model of the induction of IFN-like signal transduction by this small molecule (Fig. 21). So far, the IFNAR2 homodimer has been suggested to play various roles in IFN signal transduction [43, 55, 59], and RO8191 would induce the ISG expression via such IFNAR2 homodimer. For type I IFN, both IFNAR1 and IFNAR2 cooperate and induce phosphorylation of STATs via JAK1 and Tyk2. Conversely, for RO8191, IFNAR2 alone, as a homodimer, activates JAK1 phosphorylation and subsequent STATs activation. Experiments using siRNA and deficient cells have also shown that IFNAR1 and Tyk2 were not required to induce antiviral activity in the RO8191 compound pathway. These findings suggest a novel aspect of the IFN signaling pathway that may contribute to the understanding of other molecular signaling in IFN pathways.

RO8191 is a small molecule whose oral administration is feasible and effective in a murine model (Table 5 and Fig. 22). In the chimeric mice study, the anti-HCV effect of RO8191 and PEG-IFN was similar in that they both showed strong activity at day 1 after treatment with subsequent weak suppression of HCV replication possibly due to the immunodeficiency of chimeric mice. Further development of RO8191 by using rational chemical modifications is therefore required to produce more potent molecules for testing as an antiviral molecule which will substitute current recombinant IFN. Although RO8191 has the potential to cause IFN-like adverse effects, further development of the small-molecule agonist offers the advantages of inexpensive production cost, convenient oral administration, dose-control to reduce some adverse effects, and potentially increased activity versus current recombinant IFNs.

Whereas oral NS3 protease inhibitors in monotherapy development yield resistant viruses [25, 48], these protease inhibitors show a significantly high rate of SVR when combined with PEG-IFN [30, 60] and a NS5B polymerase inhibitor also shows additive efficacy in combination with PEG-IFN [34]. In addition to the results of the *in vivo* study, I found that RO8191 induced ISGs at a level similar to IFN-α in human primary hepatocytes (Fig. 5b); I therefore expect that RO8191 will show IFN-like activity in clinical use. As an alternative

strategy to protease/polymerase inhibitors with PEG-IFN, the combined use of these direct-acting antiviral agents with RO8191 in a new oral regimen may help overcome some of the delivery problems associated with current IFNs. SVR rates of individuals infected with HCV genotype 1 have increased from 5-20% with IFN monotherapy and up to 50% with a combination of IFN and RBV. However, the refractory patients in this therapy constitute an unmet medical need. Thus, the development of a novel IFN receptor agonist, used alone or in combination with direct-acting antiviral drugs, will add a new milestone to the treatment of chronic hepatitis C. In addition to HCV infection, type I IFNs have been approved for the treatment of multiple clinical conditions, including hairy cell leukemia, malignant melanoma, AIDS-related Kaposi's sarcoma, multiple sclerosis, and chronic hepatitis B [22]. Thus, R08191 shows strong potential as a lead compound for IFN substitutes.

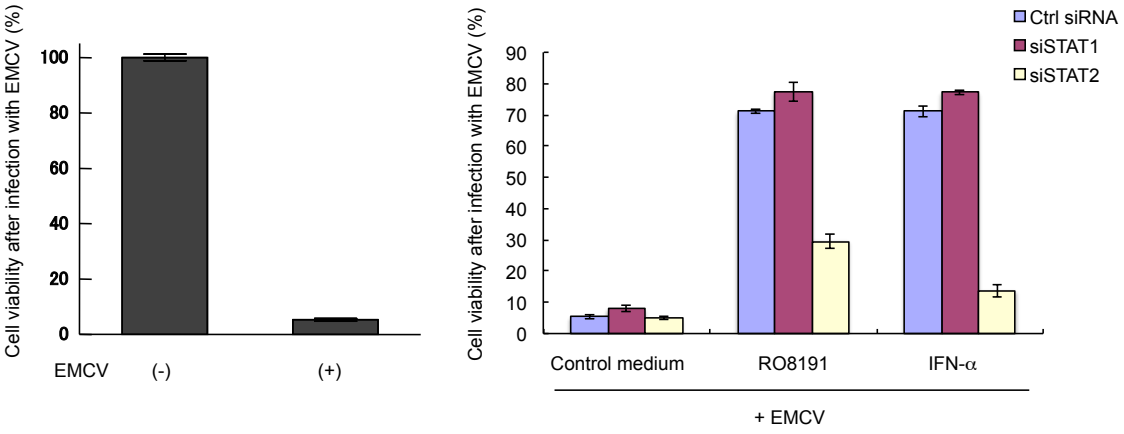

Figure 23. Anti-EMCV activity of RO8191 in STAT siRNA transfected cells.

I transfected 50 nM STAT1- or STAT2-siRNA to A549 cells, and after 72 h, I infected EMCV to the cells and treated them with 1 μM RO8191 or 2 IU/mL IFN-α. After additional 48 h incubation, I evaluated the cell viability by staining with crystal violet.

Chapter 2

Hepatic IP-10 expression is more strongly associated with liver fibrosis than IL28B single nucleotide polymorphisms in hepatocellular carcinoma resected patients with chronic hepatitis

2-1. Abstract

SNPs around IL28B and ISG expression are predictors of response to standard therapy involving IFN for chronic HCV infection. I analyzed the association between these predictors to improve the prediction of the response to IFN therapy after liver resection for HCC. Data were collected from 74 patients with HCV-induced HCC. The IL28B genotype and hepatic ISG mRNA levels were analyzed to clarify their association, focusing on the progression of liver fibrosis. Fifty patients were identified as having major alleles (rs8099917 TT) and the remaining 24 patients had minor alleles (rs8099917 TG or GG). Hepatic ISG15 expression was lower in the IL28B major group than that in the IL28B minor group ($p < 0.005$). IP-10 expression was similar between the IL28B major and minor groups ($p = 0.44$). IP-10 expression was elevated with advancing stages of liver fibrosis in HCV-infected patients ($p = 0.005$). In patients with mild or no fibrosis, the IL28B major group had lower IP-10 expression than the IL28B minor group ($p = 0.02$). However, in patients with advanced fibrosis, IP-10 expression was not different between the IL28B major and minor groups ($p = 0.66$). Hepatic ISG15 expression is associated with IL28B polymorphisms, while IP-10 is strongly affected by liver fibrosis.

2-2. Introduction

HCV infection affects 170 million people worldwide, and most acute HCV infections become chronic, with some progression to liver cirrhosis or HCC. Current standard therapy against chronic HCV infection includes PEG-IFN-α and RBV [19], which achieve a sustained SVR in only 50% of patients chronically infected with the HCV genotype 1 [17, 50, 85].

HCV infection induces IFN production via innate immune cascades [47, 65]. IFN consists of type I (IFN-α, β, and others), II (only IFN-γ), and III (IFN-λs; interleukin, or IL28A/B and IL29) IFNs, and these IFNs have antiviral activity by inducing a subset of ISGs [72]. ISGs include some genes, which show antiviral activity or are involved in lipid metabolism, apoptosis, protein degradation, and inflammation [10]. IFNs are effective against HCV infection, and are also essential for innate immunity.

Recently, a genome-wide association study showed that SNPs, located near IL28B, which encodes for IFN-λ3, are strongly associated with a virological response to IFN therapy and spontaneous clearance of HCV [18, 63, 74, 76, 77]. Especially in Japanese patients, rs8099917 is closely associated with efficacy for IFN therapy; patients with the TT genotype (termed IL28B major) have a stronger response to IFN therapy than those with TG or GG genotypes

(termed IL28B minor) [76]. Even after liver resection because of HCC [32] or liver transplantation [16], the efficacy of therapy is associated with IL28B SNP. More recently, IL28B major patients were reported to express hepatic ISGs, such as ISG15 and OAS, which were lower than those in IL28B minor patients [13, 26]. ISG expression is also known to be strongly associated with the efficacy of IFN therapy [13, 26]. However, after liver resection for HCC, the association between hepatic ISG expression and the efficacy of therapy is still unclear.

Similar to IL28B SNP, IP-10 expression is a predictor for IFN therapy, and high IP-10 expression is a predictive factor for a poor IFN response [39, 64]. Unlike other ISGs, serum IP-10 protein levels have been reported to be associated with differences in IL28B SNP [15, 40] and they also have been found not to be associated with differences in IL28B SNP [8]. IP-10 is one of the ISGs and it is regulated by inflammatory cytokines, such as TNF-α, via NF-κB transcription factor [54]. TNF-α is elevated in severe fibrosis patients [2]; therefore, IP-10 expression should be elevated in response to progression of liver fibrosis.

To clarify why IP-10 expression is not correlated with IL28B SNP, I genotyped IL28B SNP and quantitated the hepatic ISGs. I then analyzed their association, focusing on the

progression of liver fibrosis. I found that IP-10 expression is associated with IL28B SNPs only in patients with mild or no fibrosis.

2-3. Materials and Methods

Human tissue samples

Noncancerous tissue samples from 74 patients who were negative for hepatitis B virus and human immunodeficiency virus, were positive for HCV-RNA, and had undergone liver resection for hepatocellular carcinoma at the Department of Surgery and Science at Kyushu University Hospital between February 2004 and September 2010 were analyzed by genotyping, real-time RT-PCR, and immunohistochemistry. I retrospectively analyzed hepatic gene expression in these patients. For the non-B, non-C (NBNC) hepatitis group, I analyzed noncancerous tissue samples from 20 patients who were negative for hepatitis B virus, HCV, and human immunodeficiency virus, and had undergone liver resection for hepatocellular carcinoma at my institute. Samples were collected immediately after resection, as previously described [79], transported in liquid nitrogen, and stored at -80°C. The degree of chronic hepatitis in noncancerous regions was classified as follows. The degree of necroinflammatory activity (grading) was graded from A0 to A3, and the degree of fibrosis (staging) was staged as F0 to F4. Histological diagnosis of the noncancerous tissues was based on the General Rules for the Clinical and Pathological Study Group of Japan [28]. The study protocol conformed to the

ethical guidelines of the 1975 Declaration of Helsinki, and patient samples were collected after obtaining informed consent, according to an established protocol approved by the Ethics Committee of Kyushu University. The data do not contain any information that could lead to the identification of the patients.

IL28B genotyping

DNA was extracted from the patients' resected liver tissue, and genotyping was performed using Taqman GTXpress Master Mix (Life Technologies Inc., Tokyo, Japan), according to the manufacturer's protocol. The Custom TaqMan SNP Genotyping Assay (Life Technologies) was used for identifying IL28B genetic polymorphism (rs8099917).

Measurement of ISGs using real-time RT-PCR

Total RNA was extracted from resected liver tissue using reagents for RNA extraction, including ISOGEN and Ethachinmate (Nippon Gene). The synthesis of first-strand cDNA was performed using the SuperScript III First-Strand synthesis system for qRT-PCR (Life Technologies) according to the manufacturer's protocol. Real-time RT-PCR was performed

using the QuantiFast SYBR Green PCR kit (Qiagen). β-actin expression was used as the endogenous reference for each sample. The shown value was normalized using cDNA of the HCV replicon harboring HuH-7 cells, for an internal reference. Primers for each gene were designed as follows: ISG15, 5'-AGC GAA CTC ATC TTT GCC AGT ACA-3' (sense) and 5'-CAG CTC TGA CAC CGA CAT GGA-3' (antisense); OAS, 5'-GGG TGG AGT TCG ATG TGC TG-3' (sense) and 5'-GGG TTA GGT TTA TAG CCG CCA G-3' (antisense); IP-10, 5'-CTG AAT CCA GAA TCG AAG GCC ATC-3' (sense) and 5'-TGT AGG GAA GTG ATG GGA GAG G-3' (antisense); TNF, 5'-CCC AGG GAC CTC TCT CTA ATC A-3' (sense) and 5'-GCT ACA GGC TTG TCA CTC GG-3' (antisense); and β-actin, 5'-CTG GCA CCA CAC CTT CTA CAA TG-3' (sense) and 5'-GGC GTA CAG GGA TAG CAC AGG-3' (antisense).

Immunohistochemistry

Formalin-fixed, paraffin-embedded, 3-μm sections were deparaffinized in xylene, rehydrated through graded ethanol, and rinsed in phosphate-buffered saline. Heat-induced epitope retrieval was performed in 10 mM citrate buffer, pH 6.0, in a 650-Watt microwave oven at 80% output for 15 min. Endogenous peroxidase activity was blocked by incubation with

0.3% H_2O_2 for 10 min. Nonspecific antibody binding was blocked by incubating the sections with normal rabbit serum (Dako, Glostrup, Denmark) for 10 min. The sections were then incubated with anti-CXCL10 goat polyclonal antibody (1:40, R & D Systems) overnight at 4°C and labeled with the Envision Detection System (Dako) for 1 h at room temperature. The sections were then developed with 3,3' -diaminobenzidine tetrahydrochloride (DAB plus; Dako) and counterstained with 10% Mayer's acid hemalum, dehydrated, and mounted.

Cell culture and reagents

HuH-7 cells were cultured in DMEM (Life Technologies) supplemented with 10% FBS (HyClone). The HCV replicon cells were cultured in 0.5 mg/mL G418-containing DMEM supplemented with 10% FBS. The replicon construct was derived from pFK-I377neo/NS3-3'/WT, as previously described [35]. Recombinant human IFN-α2a was a kind gift from F. Hoffmann-La Roche. Recombinant human IFN-λ3 and TNF-α were purchased from R & D Systems. ISG expression in HuH-7 and HCV replicon cells was measured using total RNA that was extracted from cells cultured in the presence of 100 IU/mL IFN-α, 100 ng/mL IFN-λ3, or 1 ng/mL TNF-α for 24 h. Complementary DNA synthesis and real-time

RT-PCR reactions were performed as described above.

Statistical analysis

Pearson's χ^2 test was performed for qualitative variables. One-way analysis of variance (ANOVA), the F-test, and Student's and Welch's t-tests were performed for quantitative variables.

2-4. Results

Patient characteristics, genotyping for IL28B (rs8099917) polymorphisms, and quantification of ISG expression

Table 7 shows the patients' characteristics according to the IL28B genotype. Fifty patients were identified as having major alleles (rs8099917 TT; IL28B major). The remaining 24 patients had minor alleles (rs8099917 TG or GG; IL28B minor), and 2 of 24 patients had a minor homozygote (rs8099917 GG). I measured hepatic IP-10, ISG15, and OAS mRNA using noncancerous liver tissue, and found that ISG15 and OAS mRNA was significantly higher in IL28B minor patients than that in IL28B major patients (Fig. 24; ISG15, $p < 0.005$; OAS, $p < 0.005$). In contrast, IP-10 expression in major patients was similar to that in minor patients (Fig. 24; $p = 0.44$). Thirty-one out of 74 patients received IFN therapy prior to liver resection, and could not achieve an SVR. Table 8 shows patient characteristics according to receiving or not receiving IFN therapy.

Table 7. Patient characteristics and IL28B genotype.

Factor	IL28B SNP major (n=50)	IL28B SNP minor (n=24)	p value (univariate)
Sex, male/female	42/8	17/7	0.187
Age (years), mean ± SD	70 ± 8	70 ± 8	0.980
BMI (kg/m^2), mean ± SD	22.5 ± 3.3	22.0 ± 2.5	0.596
ALT (IU/L), mean ± SD	61.0 ± 41.5	61.0 ± 49.1	1.000
γ-GTP (IU/L), mean ± SD	72.2 ± 89.6	77.3 ± 59.5	0.774
Cholesterol (mg/dL), mean ± SD	156.8 ± 25.0	154.3 ± 26.8	0.698
Hemoglobin (g/dL), mean ± SD	13.1 ± 1.6	12.7 ± 1.9	0.311
Platelet count (x 10^4/ mL), mean ± SD	14.1 ± 4.1	13.6 ± 5.0	0.651
Fibrosis stage, F0/1/2/3/4	3/8/12/17/10	1/6/4/2/11	0.107
Activity grade, A0/1/2/3	1/13/24/12	0/5/14/5	0.900
Differentiation of hepatic cancer, (well/moderate/poor)	6/35/9	4/14/6	0.611
Tumor factor, T1/T2/T3/T4	7/26/15/2	6/12/5/1	0.652
HCV genotype, 1/2/unknown	38/8/4	16/4/4	0.516
HCV viral load (log IU/mL), mean ± SD	6.0 ± 1.1	6.1 ± 0.7	0.667

BMI, body mass index; ALT, alanine aminotransferase; γ-GTP, γ-glutamyl transpeptidase. Fibrosis stage and activity grade were classified according to the New Inuyama Classification.

Table 8. Patient characteristics and IFN therapy prior to liver resection.

Factor	IFN naïve (n=43)	IFN experienced (n=31)	p value (univariate)
Sex, male/female	35/8	24/7	0.675
Age (years), mean ± SD	71 ± 8	68 ± 7	0.153
IL28B SNP (major/minor)	31/12	19/12	0.327
IP-10 relative expression, mean ± SD	2.2 ± 2.3	2.0 ± 1.5	0.675
ISG15 relative expression, mean ± SD	1.4 ± 1.3	1.4 ± 1.5	0.953
OAS relative expression, mean ± SD	2.6 ± 0.5	2.6 ± 0.6	0.976
Fibrosis stage, F0/1/2/3/4	3/8/9/12/11	1/6/7/7/10	0.913
Activity grade, A0/1/2/3	1/7/24/11	0/11/14/6	0.245

Patient characteristics according to receiving or not receiving IFN therapy is shown.

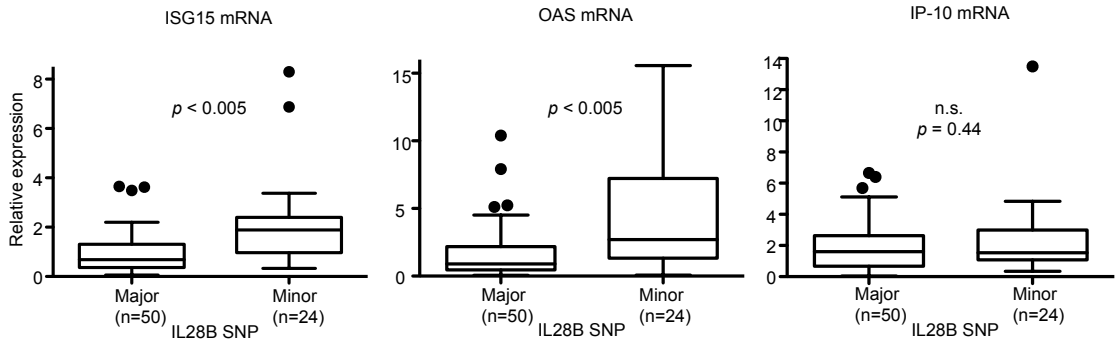

Figure 24. Comparison of hepatic gene expression levels between IL28B major and IL28B minor patients.

Expression levels of IP-10, ISG15 and OAS are shown. The p values were determined by Welch's t-test.

IP-10 expression and progression of liver fibrosis

To clarify why IP-10 is highly expressed, even in IL28B major patients, I evaluated the association between ISG expression and the stage of fibrosis. I found that IP-10 expression was significantly higher in F2/3/4 patients than that in F0/1 patients (Fig. 25; $p = 0.005$). I also separately analyzed the IL28B major and minor groups for the association between ISG expression and the stage of fibrosis. In IL28B major patients, IP-10 expression was significantly increased as the stage of fibrosis worsened (Fig. 26) (one-way ANOVA, $p = 0.03$). The one-way ANOVA analysis revealed no significant association, but tendency between other ISGs and the stage of fibrosis (ISG15, $p = 0.10$; OAS, $p = 0.09$). There were not enough IL28B minor patients for statistical analysis, but ISG expression was similar between mild and severe fibrosis patients (Fig. 26). To assess whether IP-10 expression was induced by progression of fibrosis without viral infection, I measured IP-10 expression in the liver of HCC patients with NBNC hepatitis. Progression of liver fibrosis did not induce IP-10 expression in the NBNC patients (Fig. 27a; $p = 0.32$). HCV infection induced IP-10 expression more strongly than NBNC hepatitis (Fig. 27b; $p < 0.001$). Immunohistochemistry using an anti-IP-10 antibody showed that liver sections with mild fibrosis were slightly stained. In contrast, a lot of hepatocytes were

stained in liver sections with more severe fibrosis compared with those with mild fibrosis (Fig. 28). IP-10 expression in the liver was induced by progression of fibrosis, specifically in HCV infectious patients.

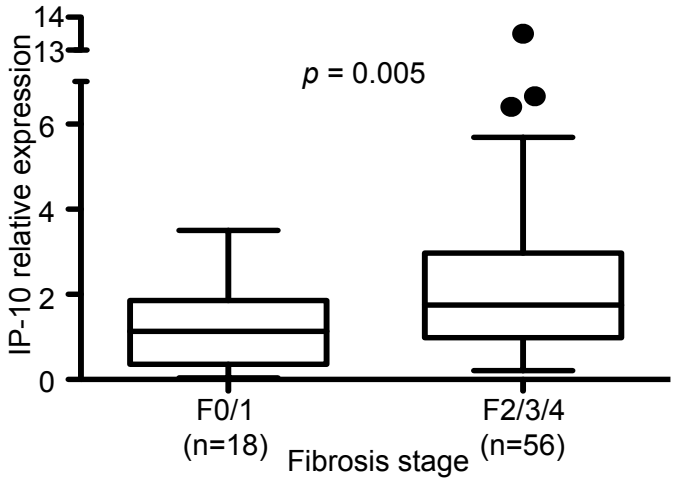

Figure 25 Comparison of hepatic IP-10 expression levels between F0/1 and F2/3/4 patients. Expression level of IP-10 in chronic hepatitis C patients. The p values were determined by Welch's t-test. Bars indicate the median of these values.

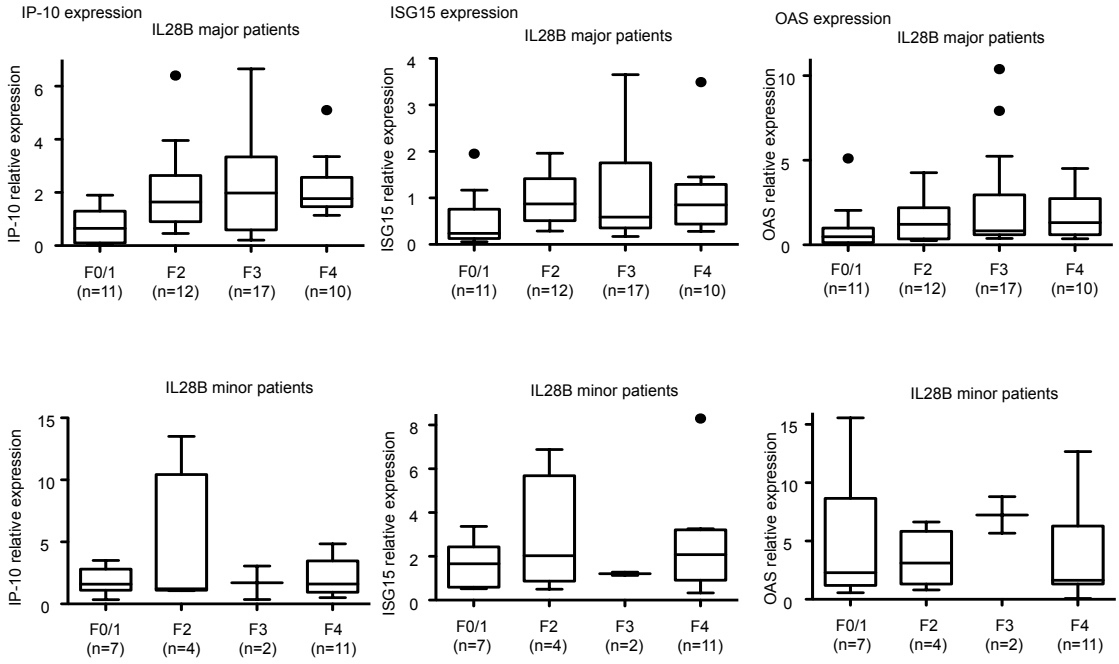

Figure 26. Comparison of hepatic ISG expression in the indicated fibrosis patients with IL28B major polymorphism (upper graphs) and IL28B minor polymorphism (lower graphs).

Bars indicate the median of these values.

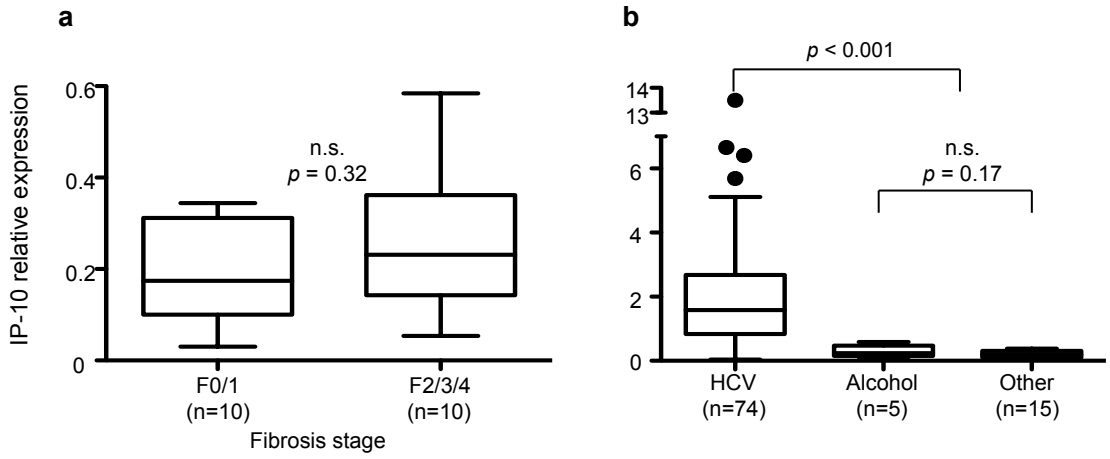

Figure 27. Comparison of hepatic IP-10 expression levels with different causes of hepatitis. (a) Expression level of IP-10 in NBNC hepatitis patients. (b) Comparison of IP-10 expression levels in patients with different causes of hepatitis: HCV, alcohol, and others. Bars indicate the median of these values. The p values were determined by Welch's t-test.

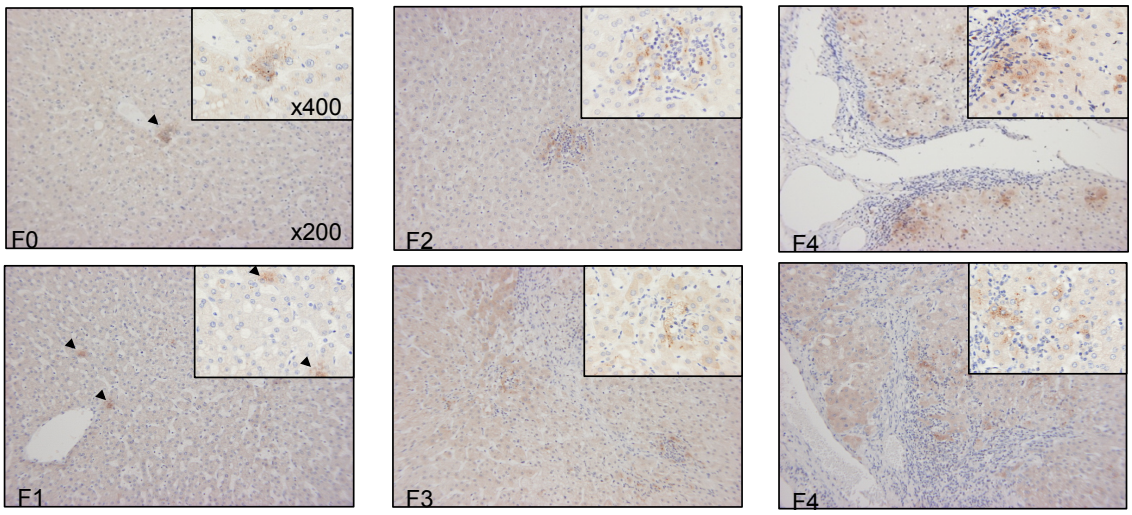

Figure 28. Comparison of hepatic IP-10 protein expression.

Hepatic IP-10 protein expression determined by immunohistochemistry is shown. Stained tissue sections from patients with differential fibrosis are shown. Arrows indicate IP-10-positive cells.

IP-10 expression and IL28B polymorphisms in mild fibrosis patients

As shown in Fig. 26, IP-10 expression was increased in the F2/3/4 stage liver compared with that in F0/1 stage liver of IL28B major patients. Therefore, to exclude an effect of progression of fibrosis on IP-10 expression, I compared IP-10 expression in IL28B SNP major and minor patients, in those with only mild or no fibrosis. In the F0/1 patients, IL28B minor patients had significantly higher IP-10 expression than IL28B major patients (Fig. 29a; $p = 0.02$), similar to ISG15 expression (Fig. 29a; $p = 0.005$). In the F2/3/4 patients, ISG15 expression in IL28B minor patients was significantly higher than that in IL28B major patients (Fig. 29b; $p = 0.03$), while IP-10 expression was not different between these patients (Fig. 29b; $p = 0.66$).

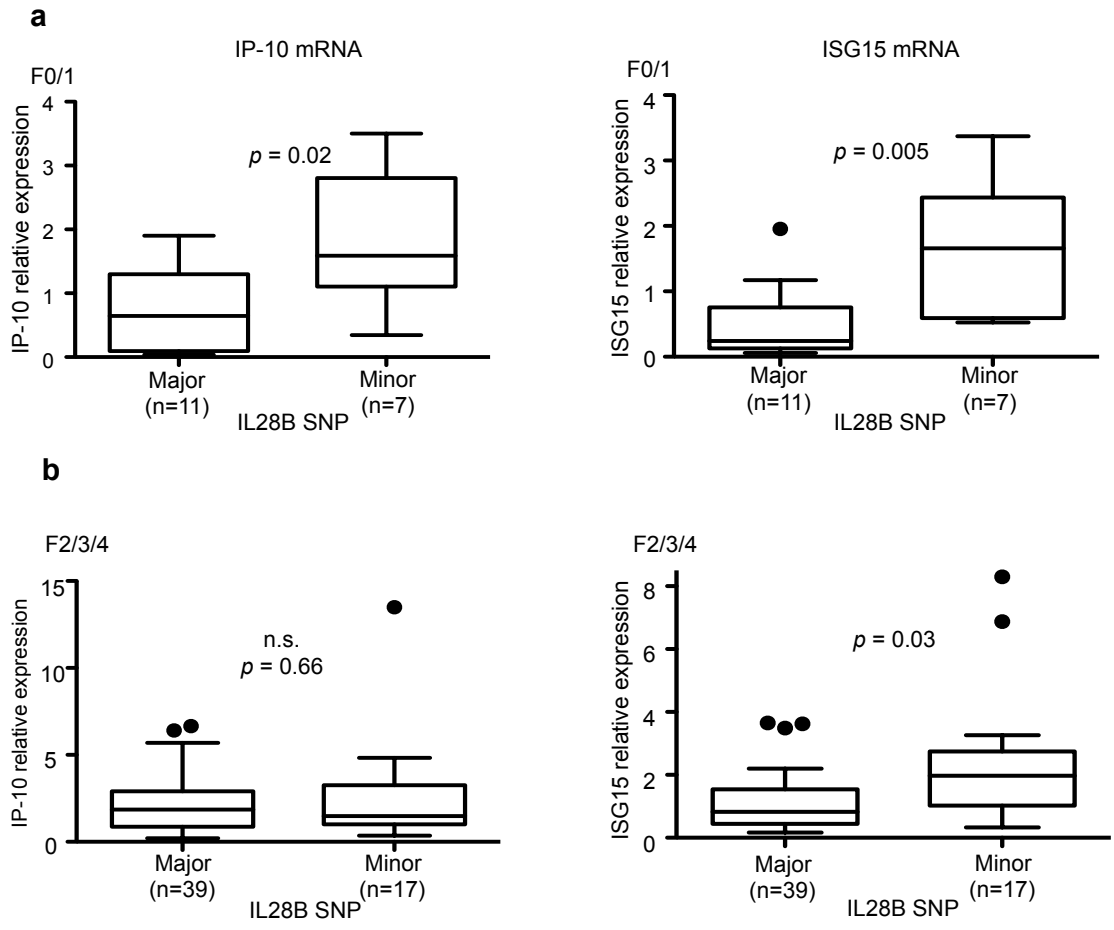

Figure 29. Comparison of hepatic IP-10 and ISG15 expression between IL28B major and IL28B minor patients in subgroups of mild or no fibrosis (a) and more progressed fibrosis (b).

Bars indicate the median of these values. The p values were determined by Welch's t-test.

Inflammatory cytokine TNF-α induces IP-10 expression in HCV RNA-replicating HuH-7 cells

I analyzed hepatic TNF mRNA expression and its association with the stage of fibrosis. TNF expression was significantly higher in F2/3/4 patients than in F0/1 patients (Fig. 30, $p = 0.02$), like IP-10 expression. IP-10 expression in the liver was mainly induced in parenchymal cells (Fig. 28). Therefore, hepatoma cell line, HuH-7 cells, and the HCV subgenomic replicon harboring HuH-7 cells were incubated with IFNs or TNF-α, to confirm the capability of IP-10 induction by these stimulators. I observed that TNF-α induced IP-10 expression much higher than type I and III IFN (Fig. 31a). ISG15 expression was also measured in the IFN- or TNF-α-treated cells. I found that ISG15 was induced by IFNs, but not by TNF-α (Fig. 31b). These results indicate that IP-10 and ISG15 expressions are separately regulated in the liver with severe fibrosis. Therefore, IP-10 expression could be used as the representative of hepatic ISGs in patients with mild or no fibrosis. However, IP-10 expression cannot be used in patients with severe fibrosis.

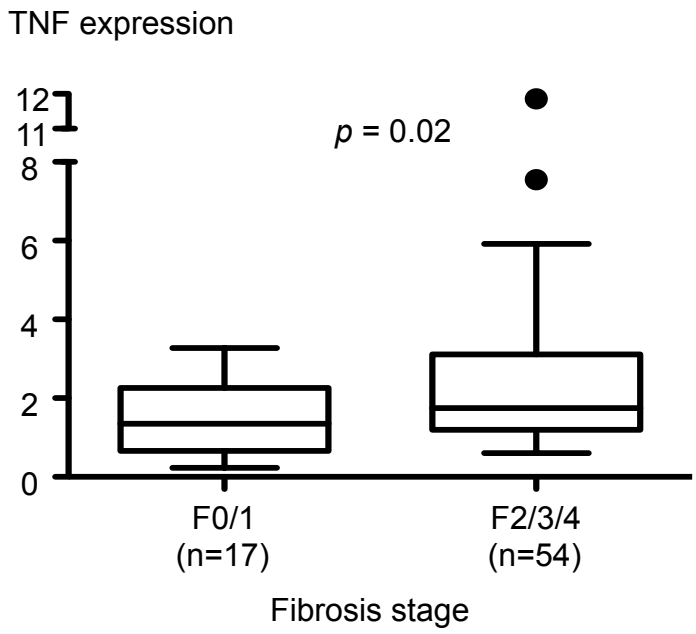

Figure 30. Comparison of hepatic TNF expression levels between F0/1 and F2/3/4 patients.

Bars indicate the median of these values. The p values were determined by Welch's t-test.

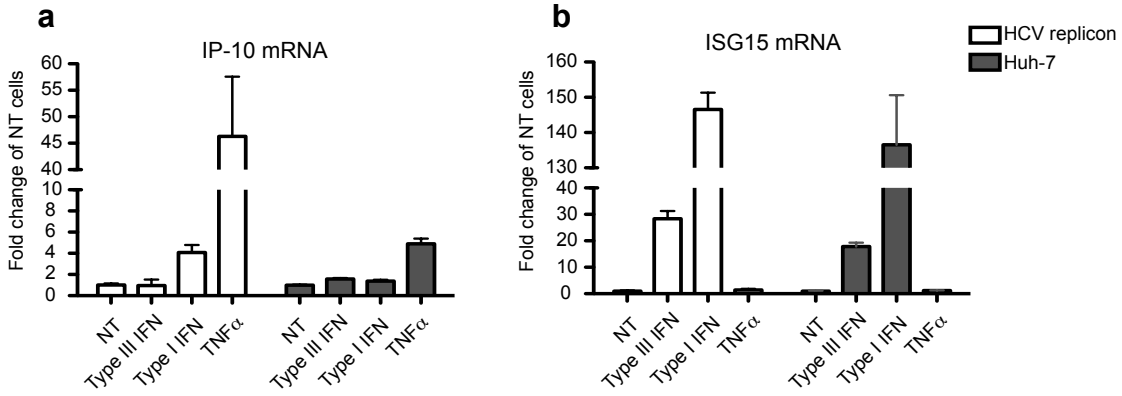

Figure 31. IP-10 (a) and ISG15 (b) expression levels were measured using real-time RT-PCR.

The values shown are the mean fold change induction compared with the mRNA level of human β-actin and the fold change induction compared with untreated cells.

2-5. Discussion

In the present study, I showed that after liver resection, ISG expression was associated with IL28B polymorphisms. IP-10 expression was significantly associated with IL28B polymorphisms in patients with mild or no fibrosis, and it was affected by the progression of fibrosis more strongly than the polymorphisms.

HCV-induced HCC occurs among patients with cirrhosis or bridging fibrosis. However, all the patients in my study were only HCC resectable patients, and therefore, patients with mild fibrosis would be selected, and the stage of fibrosis was widely distributed (Table 7). Hepatic ISG15 and OAS expressions were higher in IL28B SNP minor patients than those in IL28B SNP major patients, as previously reported [13, 26]. However, IP-10 expression was not associated with IL28B SNP (Fig. 24). Suppression of IP-10 expression during IFN therapy was reported [64], and some patients received IFN therapy prior to liver resection. The patients who had received IFN therapy prior to the resection had HCC resected at least 4 weeks after interrupting the therapy, and therefore, IP-10 expression was similar between patients who experienced IFN therapy and naïve patients (Table 8). I found that IP-10 expression was significantly higher in patients with progressed fibrosis than in those with mild or no fibrosis

(Figs. 25 and 28). IP-10 induction by progression of fibrosis complicates the association between IP-10 expression and IL28B SNP. In fact, in mild fibrosis patients, IP-10 expression was significantly higher in IL28B SNP minor patients than that in IL28B SNP major patients. However, in progressed fibrosis patients, IP-10 expression was similar among the patient groups who possessed different SNPs (Fig. 29a and b).

In chronic hepatitis C patients, TNF-α expression is elevated with progression of liver fibrosis [2]. Immunohistochemistry showed that IP-10 expression was mainly induced in hepatocytes (Fig. 28), and only a few inflammatory cells were stained (data not shown). Therefore, I evaluated the effect of TNF-α and IFNs on ISG15 and IP-10 expression in the human hepatoma cell line HuH-7 and HuH-7-derived HCV replicon cells (Fig. 31). TGF-β is also fibrosis-related cytokine, however, TGF-β did not induce IP-10 expression in the HuH-7 cells (data not shown). I found that TNF-α induced IP-10 expression is stronger than IFN signaling in these cells. These results suggest that even in the liver of IL28B SNP major and progressed fibrosis patients, TNF-α or other fibrosis-related stimulator can induce IP-10 expression. In the liver of mild fibrosis patients with IL28B minor genotype, some IL28B SNP-related stimulator would induce IP-10 expression. Thus, IP-10 expression was associated

with IL28B SNP only in patients with mild or no fibrosis. In contrast, ISG15 was not induced by TNF-α, suggesting that ISG15 is strongly regulated by IFNs (Fig. 31b). Therefore, irrespective of progression of fibrosis, ISG15 expression is higher in IL28B SNP minor patients than that in IL28B SNP major patients (Fig. 29).

In the NBNC patients, IP-10 expression was rarely induced by progression of fibrosis and was much lower than that in HCV infectious patients (Fig. 27b). It is reported that patients infected with HCV infected patients, rather than HBV, expressed higher IP-10 [2, 56]. At least in clinical, IP-10 induction would dramatically occur by HCV infection, and may be quiescent without any viral infection. Thus, IP-10 expression in the NBNC patients could be scarcely induced, or be near the detection limit. With TNF-α stimulation, HCV replicon cells expressed IP-10 mRNA more strongly than HCV RNA negative HuH-7 cells. These data suggest that IP-10 induction by fibrosis-related stimulation could be enhanced by HCV infection or replication. Recently, Thomas *et al.* showed that HCV infection induces IFN-λ expression in the liver of chimpanzees [78]. IFN-λ and fibrosis-related stimulations could induce IP-10 expression coordinately.

I then evaluated whether IP-10 expression can predicte therapeutic outcomes. IL28B SNP

is associated with IFN therapy outcomes, especially among 54 HCV genotype 1 infected patients. Thirty-six patients did not received IFN therapy; 19 patients due to low platelet counts, 11 patients, due to tumor recurrence, and 6 patients rejected the therapy. Eighteen patients with genotype 1 infection were administered PEG-IFN-α2b and RBV combination therapy for 48 weeks after liver resection. IL28B SNP was significantly associated with IFN therapeutic outcome, and the hepatic mRNA expressions of ISG15 and OAS at resection were significantly lower in the SVR group than those in the non-SVR group (data not shown). However, IP-10 expression was not associated with the outcome. Lagging *et al.* [40] and Fattovich *et al.* [15] reported that serum IP-10 protein levels are higher in IL28B SNP minor patients than those in IL28B SNP major patients. Liver fibrosis of the patients in their study was less severe than that in the patients in my study. A correlation between hepatic IP-10 expression and serum IP-10 protein levels was reported by Askarieh *et al.* [1], and hepatic and serum IP-10 expression has been reported as a predictor of IFN therapy outcome [39, 64]. However, IP-10 expression as a predictor of outcome would not be beneficial in patients with severe fibrosis. Therefore, to predict efficacy using IP-10 expression, progression of fibrosis should be considered.

The mechanism of how IL28B SNP minor patients express excessive ISGs is unclear.

Excessive and probably maximal ISG expression before treatment would prevent the activity of IFN. Sugiyama *et al.* showed that long TA repeats in the promoter region of IL28B possess strong IL28B induction capability [73]. While, Smith *et al.* reported that IL28B polymorphism affects methylation in the transcription factor binding sites and results in high IL28B expression in IL28B SNP minor patients [70]. IL28B and IFN-λ3 have antiviral activity, and PEG-IFN-λ has been previously used in a clinical trial [52]. However, an association between PEG-IFN-λ efficacy and IL28B SNP has not been reported. Investigation of PEG-IFN-λ efficacy in IL28B SNP minor patients may help clarify the function of IFN-λ in HCV infection. Further studies are required to determine this issue, and this could improve the health of chronic HCV-infected patients.

General Discussion

I identified a novel small molecule that acts like IFN by directly interacting with the type I IFN receptor to drive ISG expression, shown in chapter 1. RO8191, used in combination with direct-acting antiviral drugs, will add a new oral option against chronic hepatitis C infection. IFN-α and RO8191 share similar gene induction, therefore, RO8191 may cause adverse event similar to IFN-α. RO8191 have a potential to be administered orally, and may be easier to control the daily dosage than IFN-α that is administered weekly. Severe adverse events caused by RO8191 treatment may be avoided by controlling the dosage.

I also found that RO8191 showed anti-HCV activity even in IFNAR1 or Tyk2 siRNA transfected cells, unlike IFN. These results were consistent with ISGs induction in IFNAR1 or Tyk2 deficient cells. In addition to antiviral effect, IFN showed an activation to immune cells and suppressor effect to tumor cells. To clarify whether IFNAR1 or Tyk2 contributes those effects by IFN, immune activation and cellular growth inhibitory effect by RO8191 is assessed. Further evaluations are needed to reveal novel molecular mechanism of IFN signaling.

The association between IL28B SNP and clinical outcomes had been reported, and in chapter 2, I analyzed the association among IL28B SNP, IP-10 expression, other ISG expression

and liver fibrosis (Fig. 32), although, the mechanism underlying the association was unclear. Most recently, Prokunina-Olsson *et al.* reported that IFNL4 ss469415590 genetic polymorphism, TT or ΔG, is significantly associated with the IFN therapeutic outcome [61]. ss469415590 is located in the exon region of the IFNL4 gene, therefore, the ΔG allele leads to a translational frameshift. Patients with this ΔG allele in ss469415590 express a novel IFN-like antiviral IFNL4 gene; while, patients with a TT homozygous haplotype express an unknown gene without antiviral function. Prokunina-Olsson *et al.* also reported that IFNL4 ΔG would inhibit IFN-involving therapy. Most Japanese individuals who had rs8099917 risk alleles also had ss469415590 risk ΔG alleles [37], indicating IL28B risk allele is associated with the expression of functional IFNL4.

Some ISGs, such as ISG15 and USP18, have been reported to inhibit IFN activity and help HCV replication [5, 6, 62, 68], and the expression of ISGs have been reported as a predictor of the possible response to IFN therapy. ISG15 and USP18 expression levels were also correlated with IFNL4 ΔG expression [37]. These ISGs' expression levels would be induced by IFNL4, indicating that the rs8099917 polymorphism risk allele reflects the presence of the antiviral IFNL4 gene; and that ISGs' expression levels are affected by IFNL4 expression levels.

Therefore, patients with the ΔG risk allele cannot respond to IFN therapy (Fig. 33). To clarify whether RO8191 shows an efficacy to the patients with IL28B/IFNL4 risk allele, evaluation of RO8191 using the cells that expresses high inhibitory ISGs is needed. SOCS1 is also reported as negative regulator of IFN signaling [3], like ISG15 and USP18. Mechanism that inhibits IFN signal by these inhibitory ISGs is still unclear. RO8191 activity is independent of IFNAR1/Tyk2, therefore, RO8191 signaling may not be inhibited by those inhibitory ISGs. Thus, nonresponders by current therapy may be cured by RO8191-including therapy in future.

In conclusion, RO8191 is novel small molecule that activates IFN signaling directly, and RO8191 would contribute a development of novel treatment to various diseases, including chronic hepatitis C patients with IL28B/IFNL4 unfavorable genotype.

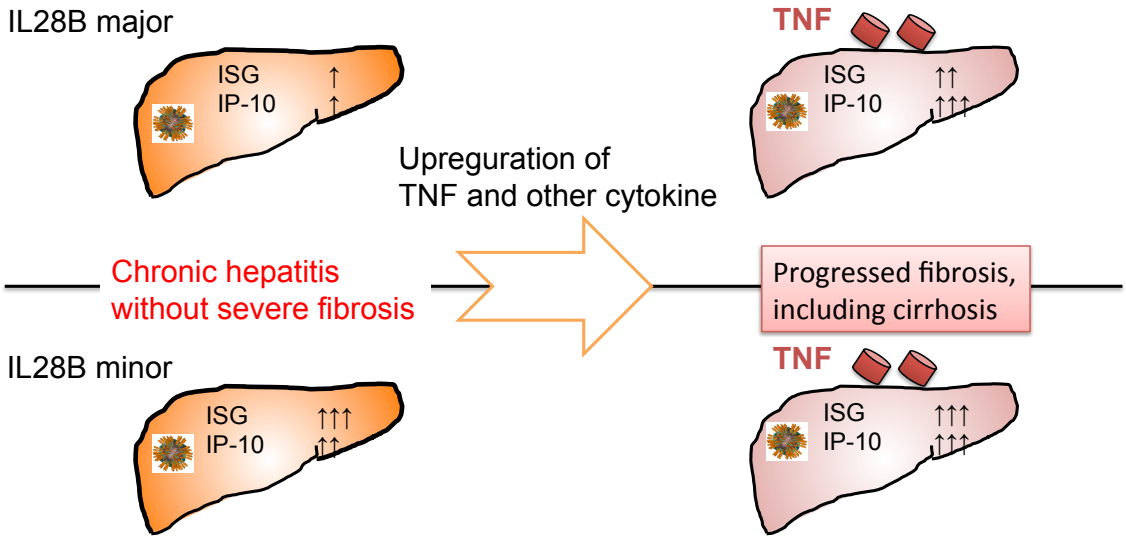

Figure 32. A schematic summary of the results reported in chapter 2.

The association among IL28B SNP, IP-10 expression, other ISG expression and liver fibrosis is shown.

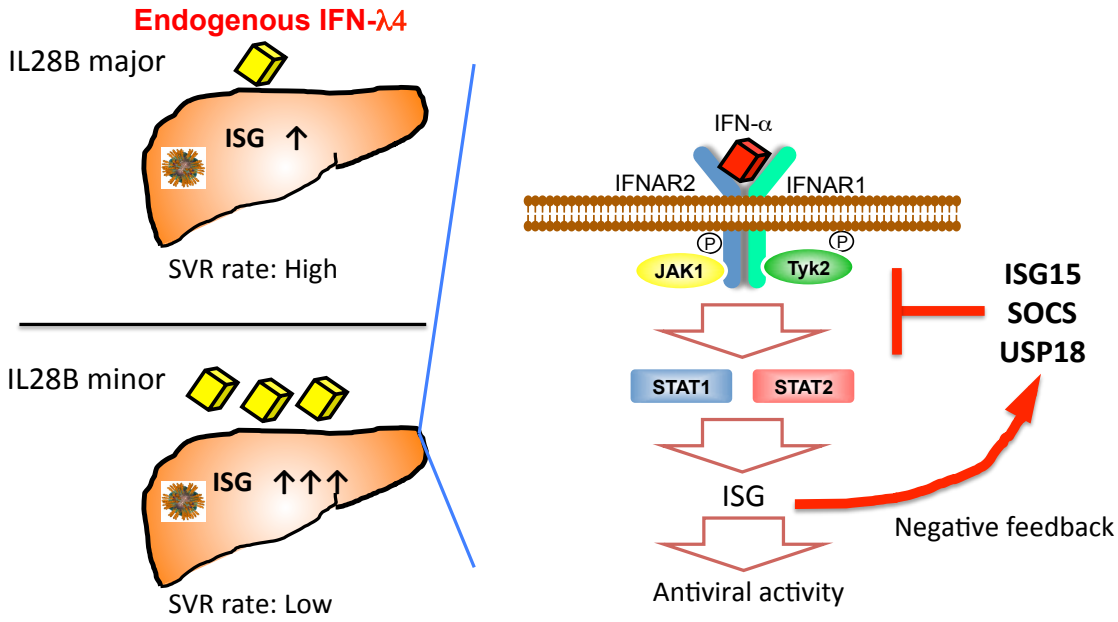

Figure 33. A schematic showing the possible mechanism of IFN-α pathway inhibition in the liver of patients with IL28B/IFNL4 minor SNP.

Hepatic ISGs' expressions in the chronic HCV infection are induced by IFNL4, indicating that the rs8099917 polymorphism risk allele reflects the presence of the antiviral IFNL4 gene. Patients with the IL28B risk allele cannot respond to IFN therapy due to high expression of inhibitory ISGs.

Acknowledgements

I deeply appreciate Dr. Kazuichi Sakamoto for his helpful advices and critical review of all of the manuscripts.

I am grateful to Prof. George Stark for providing me the 2fTGH, U1A and U5A cell lines, and Prof. Akinori Takaoka for mouse Ifnar1-knockout MEFs. I also thank Isamu Kusanagi and Chiaki Tanaka for technical assistance, AVSS Co., Ltd. for technical assistance on EMCV, and Editing Services at Chugai Pharmaceutical Co., Ltd. for editorial assistance.

The study in chapter 2 was supported by a Grant-in-Aid from the Ministry of Health, Labour and Welfare, Japan (H23-kannen-003).

References

[1] Askarieh G, Alsio A, Pugnale P, Negro F, Ferrari C, Neumann AU*, et al.* **Systemic and intrahepatic interferon-gamma-inducible protein 10 kDa predicts the first-phase decline in hepatitis C virus RNA and overall viral response to therapy in chronic hepatitis C**. *Hepatology*. 2010;51(5):1523-30.

[2] Bieche I, Asselah T, Laurendeau I, Vidaud D, Degot C, Paradis V*, et al.* **Molecular profiling of early stage liver fibrosis in patients with chronic hepatitis C virus infection**. *Virology*. 2005;332(1):130-44.

[3] Brand S, Zitzmann K, Dambacher J, Beigel F, Olszak T, Vlotides G*, et al.* **SOCS-1 inhibits expression of the antiviral proteins 2',5'-OAS and MxA induced by the novel interferon-lambdas IL-28A and IL-29**. *Biochemical and biophysical research communications*. 2005;331(2):543-8.

[4] Chen HM, Tanaka N, Mitani Y, Oda E, Nozawa H, Chen JZ*, et al.* **Critical role for constitutive type I interferon signaling in the prevention of cellular transformation**. *Cancer science*. 2009;100(3):449-56.

[5] Chen L, Sun J, Meng L, Heathcote J, Edwards AM, McGilvray ID. **ISG15, a ubiquitin-like interferon-stimulated gene, promotes hepatitis C virus production in vitro: implications for chronic infection and response to treatment**. *J Gen Virol*. 2010;91(Pt 2):382-8.

[6] Chen L, Li S, McGilvray I. **The ISG15/USP18 ubiquitin-like pathway (ISGylation system) in hepatitis C virus infection and resistance to interferon therapy**. *Int J Biochem Cell Biol*. 2011;43(10):1427-31.

[7] Czepiel J, Biesiada G, Mach T. **Viral hepatitis C**. *Polskie Archiwum Medycyny Wewnetrznej*. 2008;118(12):734-40.

[8] Darling JM, Aerssens J, Fanning G, McHutchison JG, Goldstein DB, Thompson AJ*, et al.* **Quantitation of pretreatment serum interferon-gamma-inducible protein-10 improves the**

predictive value of an IL28B gene polymorphism for hepatitis C treatment response. *Hepatology*. 2011;53(1):14-22.

[9] Dash S, Prabhu R, Hazari S, Bastian F, Garry R, Zou W, *et al.* **Interferons alpha, beta, gamma each inhibit hepatitis C virus replication at the level of internal ribosome entry site-mediated translation**. *Liver international : official journal of the International Association for the Study of the Liver*. 2005;25(3):580-94.

[10] de Veer MJ, Holko M, Frevel M, Walker E, Der S, Paranjape JM, *et al.* **Functional classification of interferon-stimulated genes identified using microarrays**. *Journal of leukocyte biology*. 2001;69(6):912-20.

[11] Der SD, Zhou A, Williams BR, Silverman RH. **Identification of genes differentially regulated by interferon alpha, beta, or gamma using oligonucleotide arrays**. *Proceedings of the National Academy of Sciences of the United States of America*. 1998;95(26):15623-8.

[12] Diaz MO, Ziemin S, Le Beau MM, Pitha P, Smith SD, Chilcote RR, *et al.* **Homozygous deletion of the alpha- and beta 1-interferon genes in human leukemia and derived cell lines**. *Proceedings of the National Academy of Sciences of the United States of America*. 1988;85(14):5259-63.

[13] Dill MT, Duong FH, Vogt JE, Bibert S, Bochud PY, Terracciano L, *et al.* **Interferon-induced gene expression is a stronger predictor of treatment response than IL28B genotype in patients with hepatitis C**. *Gastroenterology*. 2011;140(3):1021-31.

[14] Farnsworth A, Flaman AS, Prasad SS, Gravel C, Williams A, Yauk CL, *et al.* **Acetaminophen modulates the transcriptional response to recombinant interferon-beta**. *PloS one*. 2010;5(6):e11031.

[15] Fattovich G, Covolo L, Bibert S, Askarieh G, Lagging M, Clement S, *et al.* **IL28B polymorphisms, IP-10 and viral load predict virological response to therapy in chronic hepatitis C**. *Aliment Pharmacol Ther*. 2011;33(10):1162-72.

[16] Fukuhara T, Taketomi A, Motomura T, Okano S, Ninomiya A, Abe T, *et al.* **Variants in IL28B in liver recipients and donors correlate**

with response to peg-interferon and ribavirin therapy for recurrent hepatitis C. *Gastroenterology*. 2010;139(5):1577-85, 85 e1-3.

[17] Fukuhara T, Taketomi A, Okano S, Ikegami T, Soejima Y, Shirabe K*, et al.* **Mutations in hepatitis C virus genotype 1b and the sensitivity of interferon-ribavirin therapy after liver transplantation**. *J Hepatol*. 2010;52(5):672-80.

[18] Ge D, Fellay J, Thompson AJ, Simon JS, Shianna KV, Urban TJ*, et al.* **Genetic variation in IL28B predicts hepatitis C treatment-induced viral clearance**. *Nature*. 2009;461(7262):399-401.

[19] Ghany MG, Strader DB, Thomas DL, Seeff LB. **Diagnosis, management, and treatment of hepatitis C: an update**. *Hepatology*. 2009;49(4):1335-74.

[20] Ghislain JJ, Fish EN. **Application of genomic DNA affinity chromatography identifies multiple interferon-alpha-regulated Stat2 complexes**. *The Journal of biological chemistry*. 1996;271(21):12408-13.

[21] Gupta S, Jiang M, Pernis AB. **IFN-alpha activates Stat6 and leads to the formation of Stat2:Stat6 complexes in B cells**. *Journal of immunology*. 1999;163(7):3834-41.

[22] Gutterman JU. **Cytokine therapeutics: lessons from interferon alpha**. *Proceedings of the National Academy of Sciences of the United States of America*. 1994;91(4):1198-205.

[23] Hemmi H, Takeuchi O, Kawai T, Kaisho T, Sato S, Sanjo H*, et al.* **A Toll-like receptor recognizes bacterial DNA**. *Nature*. 2000;408(6813):740-5.

[24] Hemmi H, Kaisho T, Takeuchi O, Sato S, Sanjo H, Hoshino K*, et al.* **Small anti-viral compounds activate immune cells via the TLR7 MyD88-dependent signaling pathway**. *Nature immunology*. 2002;3(2):196-200.

[25] Hezode C, Forestier N, Dusheiko G, Ferenci P, Pol S, Goeser T*, et al.* **Telaprevir and peginterferon with or without ribavirin for**

chronic HCV infection. *The New England journal of medicine*. 2009;360(18):1839-50.

[26] Honda M, Sakai A, Yamashita T, Nakamoto Y, Mizukoshi E, Sakai Y*, et al.* **Hepatic ISG expression is associated with genetic variation in interleukin 28B and the outcome of IFN therapy for chronic hepatitis C**. *Gastroenterology*. 2010;139(2):499-509.

[27] Hoshino K, Takeuchi O, Kawai T, Sanjo H, Ogawa T, Takeda Y*, et al.* **Cutting edge: Toll-like receptor 4 (TLR4)-deficient mice are hyporesponsive to lipopolysaccharide: evidence for TLR4 as the Lps gene product**. *Journal of immunology*. 1999;162(7):3749-52.

[28] Ichida F, Tsuji T, Omata M, Ichida T, Inoue K, Kamimura T*, et al.* **New Inuyama classification; New criteria for histological assessment of chronic hepatitis**. *International Hepatology Communications*. 1996;6(2):112-9.

[29] Inoue K, Umehara T, Ruegg UT, Yasui F, Watanabe T, Yasuda H*, et al.* **Evaluation of a cyclophilin inhibitor in hepatitis C virus-infected chimeric mice in vivo**. *Hepatology*. 2007;45(4):921-8.

[30] Jacobson IM, McHutchison JG, Dusheiko G, Di Bisceglie AM, Reddy KR, Bzowej NH*, et al.* **Telaprevir for previously untreated chronic hepatitis C virus infection**. *The New England journal of medicine*. 2011;364(25):2405-16.

[31] Kawai T, Akira S. **Toll-like receptor and RIG-I-like receptor signaling**. *Annals of the New York Academy of Sciences*. 2008;1143:1-20.

[32] Kawaoka T, Aikata H, Takaki S, Hiramatsu A, Waki K, Hiraga N*, et al.* **IL28B polymorphism may guide pegylated interferon plus ribavirin therapy even after curative treatment for hepatitis C virus-related hepatocellular carcinoma**. *Journal of viral hepatitis*. 2011;18(10):e550-60.

[33] Kneteman NM, Weiner AJ, O'Connell J, Collett M, Gao T, Aukerman L*, et al.* **Anti-HCV therapies in chimeric scid-Alb/uPA mice parallel outcomes in human clinical application**. *Hepatology*. 2006;43(6):1346-53.

[34] Kneteman NM, Howe AY, Gao T, Lewis J, Pevear D, Lund G, *et al.* **HCV796: A selective nonstructural protein 5B polymerase inhibitor with potent anti-hepatitis C virus activity in vitro, in mice with chimeric human livers, and in humans infected with hepatitis C virus**. *Hepatology*. 2009;49(3):745-52.

[35] Konishi H, Okamoto K, Ohmori Y, Yoshino H, Ohmori H, Ashihara M, *et al.* **An orally available, small-molecule interferon inhibits viral replication**. *Scientific reports*. 2012;2:259.

[36] Konishi H, Shirabe K, Yoshiya S, Ikeda T, Ikegami T, Yoshizumi T, *et al.* **Hepatic interferon-gamma-induced protein-10 expression is more strongly associated with liver fibrosis than interleukin-28B single nucleotide polymorphisms in hepatocellular carcinoma resected patients with chronic hepatitis C**. *Hepatology research : the official journal of the Japan Society of Hepatology*. 2013;43(11):1139-47.

[37] Konishi H, Motomura T, Matsumoto Y, Harimoto N, Ikegami T, Yoshizumi T, *et al.* **Interferon-lambda4 genetic polymorphism is associated with the therapy response for hepatitis C virus recurrence after a living donor liver transplant**. *Journal of viral hepatitis*. 2014;21(6):397-404.

[38] Kwong AD, McNair L, Jacobson I, George S. **Recent progress in the development of selected hepatitis C virus NS3.4A protease and NS5B polymerase inhibitors**. *Current opinion in pharmacology*. 2008;8(5):522-31.

[39] Lagging M, Romero AI, Westin J, Norkrans G, Dhillon AP, Pawlotsky JM, *et al.* **IP-10 predicts viral response and therapeutic outcome in difficult-to-treat patients with HCV genotype 1 infection**. *Hepatology*. 2006;44(6):1617-25.

[40] Lagging M, Askarieh G, Negro F, Bibert S, Soderholm J, Westin J, *et al.* **Response prediction in chronic hepatitis C by assessment of IP-10 and IL28B-related single nucleotide polymorphisms**. *PloS one*. 2011;6(2):e17232.

[41] Lavanchy D. **The global burden of hepatitis C**. *Liver international :*

official journal of the International Association for the Study of the Liver. 2009;29 Suppl 1:74-81.

[42] Leung S, Qureshi SA, Kerr IM, Darnell JE, Jr., Stark GR. **Role of STAT2 in the alpha interferon signaling pathway**. *Molecular and cellular biology*. 1995;15(3):1312-7.

[43] Lewerenz M, Mogensen KE, Uze G. **Shared receptor components but distinct complexes for alpha and beta interferons**. *Journal of molecular biology*. 1998;282(3):585-99.

[44] Li X, Leung S, Qureshi S, Darnell JE, Jr., Stark GR. **Formation of STAT1-STAT2 heterodimers and their role in the activation of IRF-1 gene transcription by interferon-alpha**. *The Journal of biological chemistry*. 1996;271(10):5790-4.

[45] Lohmann V, Korner F, Koch J, Herian U, Theilmann L, Bartenschlager R. **Replication of subgenomic hepatitis C virus RNAs in a hepatoma cell line**. *Science*. 1999;285(5424):110-3.

[46] Lutfalla G, Holland SJ, Cinato E, Monneron D, Reboul J, Rogers NC*, et al.* **Mutant U5A cells are complemented by an interferon-alpha beta receptor subunit generated by alternative processing of a new member of a cytokine receptor gene cluster**. *The EMBO journal*. 1995;14(20):5100-8.

[47] Marukian S, Andrus L, Sheahan TP, Jones CT, Charles ED, Ploss A*, et al.* **Hepatitis C virus induces interferon-lambda and interferon-stimulated genes in primary liver cultures**. *Hepatology*. 2011;54(6):1913-23.

[48] McHutchison JG, Everson GT, Gordon SC, Jacobson IM, Sulkowski M, Kauffman R*, et al.* **Telaprevir with peginterferon and ribavirin for chronic HCV genotype 1 infection**. *The New England journal of medicine*. 2009;360(18):1827-38.

[49] Mercer DF, Schiller DE, Elliott JF, Douglas DN, Hao C, Rinfret A*, et al.* **Hepatitis C virus replication in mice with chimeric human livers**. *Nature medicine*. 2001;7(8):927-33.

[50] Morita K, Taketomi A, Shirabe K, Umeda K, Kayashima H, Ninomiya M*, et al.* **Clinical significance and potential of hepatic**

microRNA-122 expression in hepatitis C. *Liver international : official journal of the International Association for the Study of the Liver*. 2011;31(4):474-84.

[51] Mosca JD, Pitha PM. **Transcriptional and posttranscriptional regulation of exogenous human beta interferon gene in simian cells defective in interferon synthesis**. *Molecular and cellular biology*. 1986;6(6):2279-83.

[52] Muir AJ, Shiffman ML, Zaman A, Yoffe B, de la Torre A, Flamm S*, et al.* **Phase 1b study of pegylated interferon lambda 1 with or without ribavirin in patients with chronic genotype 1 hepatitis C virus infection**. *Hepatology*. 2010;52(3):822-32.

[53] Novick D, Cohen B, Rubinstein M. **The human interferon alpha/beta receptor: characterization and molecular cloning**. *Cell*. 1994;77(3):391-400.

[54] Ohmori Y, Hamilton TA. **The interferon-stimulated response element and a kappa B site mediate synergistic induction of murine IP-10 gene transcription by IFN-gamma and TNF-alpha**. *Journal of immunology*. 1995;154(10):5235-44.

[55] Pattyn E, Van Ostade X, Schauvliege L, Verhee A, Kalai M, Vandekerckhove J*, et al.* **Dimerization of the interferon type I receptor IFNaR2-2 is sufficient for induction of interferon effector genes but not for full antiviral activity**. *The Journal of biological chemistry*. 1999;274(49):34838-45.

[56] Patzwahl R, Meier V, Ramadori G, Mihm S. **Enhanced expression of interferon-regulated genes in the liver of patients with chronic hepatitis C virus infection: detection by suppression-subtractive hybridization**. *J Virol*. 2001;75(3):1332-8.

[57] Perry ST, Buck MD, Lada SM, Schindler C, Shresta S. **STAT2 mediates innate immunity to Dengue virus in the absence of STAT1 via the type I interferon receptor**. *PLoS pathogens*. 2011;7(2):e1001297.

[58] Pestka S, Langer JA, Zoon KC, Samuel CE. **Interferons and their actions**. *Annual review of biochemistry*. 1987;56:727-77.

[59] Platis D, Foster GR. **Activity of hybrid type I interferons in cells lacking Tyk2: a common region of IFN-alpha 8 induces a response, but IFN-alpha2/8 hybrids can behave like IFN-beta**. *Journal of interferon & cytokine research : the official journal of the International Society for Interferon and Cytokine Research*. 2003;23(11):655-66.

[60] Poordad F, McCone J, Jr., Bacon BR, Bruno S, Manns MP, Sulkowski MS*, et al.* **Boceprevir for untreated chronic HCV genotype 1 infection**. *The New England journal of medicine*. 2011;364(13):1195-206.

[61] Prokunina-Olsson L, Muchmore B, Tang W, Pfeiffer RM, Park H, Dickensheets H*, et al.* **A variant upstream of IFNL3 (IL28B) creating a new interferon gene IFNL4 is associated with impaired clearance of hepatitis C virus**. *Nature genetics*. 2013;45(2):164-71.

[62] Randall G, Chen L, Panis M, Fischer AK, Lindenbach BD, Sun J*, et al.* **Silencing of USP18 potentiates the antiviral activity of interferon against hepatitis C virus infection**. *Gastroenterology*. 2006;131(5):1584-91.

[63] Rauch A, Kutalik Z, Descombes P, Cai T, Di Iulio J, Mueller T*, et al.* **Genetic variation in IL28B is associated with chronic hepatitis C and treatment failure: a genome-wide association study**. *Gastroenterology*. 2010;138(4):1338-45, 45 e1-7.

[64] Romero AI, Lagging M, Westin J, Dhillon AP, Dustin LB, Pawlotsky JM*, et al.* **Interferon (IFN)-gamma-inducible protein-10: association with histological results, viral kinetics, and outcome during treatment with pegylated IFN-alpha 2a and ribavirin for chronic hepatitis C virus infection**. *The Journal of infectious diseases*. 2006;194(7):895-903.

[65] Saito T, Owen DM, Jiang F, Marcotrigiano J, Gale M, Jr. **Innate immunity induced by composition-dependent RIG-I recognition of hepatitis C virus RNA**. *Nature*. 2008;454(7203):523-7.

[66] Sakamoto H, Okamoto K, Aoki M, Kato H, Katsume A, Ohta A, *et al.* **Host sphingolipid biosynthesis as a target for hepatitis C virus therapy**. *Nature chemical biology*. 2005;1(6):333-7.

[67] Sarasin-Filipowicz M, Oakeley EJ, Duong FH, Christen V, Terracciano L, Filipowicz W, *et al.* **Interferon signaling and treatment outcome in chronic hepatitis C**. *Proceedings of the National Academy of Sciences of the United States of America*. 2008;105(19):7034-9.

[68] Sarasin-Filipowicz M, Wang X, Yan M, Duong FH, Poli V, Hilton DJ, *et al.* **Alpha interferon induces long-lasting refractoriness of JAK-STAT signaling in the mouse liver through induction of USP18/UBP43**. *Molecular and cellular biology*. 2009;29(17):4841-51.

[69] Shuai K, Horvath CM, Huang LH, Qureshi SA, Cowburn D, Darnell JE, Jr. **Interferon activation of the transcription factor Stat91 involves dimerization through SH2-phosphotyrosyl peptide interactions**. *Cell*. 1994;76(5):821-8.

[70] Smith KR, Suppiah V, O'Connor K, Berg T, Weltman M, Abate ML, *et al.* **Identification of improved IL28B SNPs and haplotypes for prediction of drug response in treatment of hepatitis C using massively parallel sequencing in a cross-sectional European cohort**. *Genome Med*. 2011;3(8):57.

[71] Stark GR, Kerr IM, Williams BR, Silverman RH, Schreiber RD. **How cells respond to interferons**. *Annual review of biochemistry*. 1998;67:227-64.

[72] Stark GR. **How cells respond to interferons revisited: from early history to current complexity**. *Cytokine & growth factor reviews*. 2007;18(5-6):419-23.

[73] Sugiyama M, Tanaka Y, Wakita T, Nakanishi M, Mizokami M. **Genetic variation of the IL-28B promoter affecting gene expression**. *PloS one*. 2011;6(10):e26620.

[74] Suppiah V, Moldovan M, Ahlenstiel G, Berg T, Weltman M, Abate ML, *et al.* **IL28B is associated with response to chronic hepatitis C interferon-alpha and ribavirin therapy**. *Nature genetics*.

2009;41(10):1100-4.

[75] Takeuchi T, Katsume A, Tanaka T, Abe A, Inoue K, Tsukiyama-Kohara K, *et al.* **Real-time detection system for quantification of hepatitis C virus genome**. *Gastroenterology*. 1999;116(3):636-42.

[76] Tanaka Y, Nishida N, Sugiyama M, Kurosaki M, Matsuura K, Sakamoto N, *et al.* **Genome-wide association of IL28B with response to pegylated interferon-alpha and ribavirin therapy for chronic hepatitis C**. *Nature genetics*. 2009;41(10):1105-9.

[77] Thomas DL, Thio CL, Martin MP, Qi Y, Ge D, O'Huigin C, *et al.* **Genetic variation in IL28B and spontaneous clearance of hepatitis C virus**. *Nature*. 2009;461(7265):798-801.

[78] Thomas E, Gonzalez VD, Li Q, Modi AA, Chen W, Noureddin M, *et al.* **HCV infection induces a unique hepatic innate immune response associated with robust production of type III interferons**. *Gastroenterology*. 2012;142(4):978-88.

[79] Toshima T, Shirabe K, Takeishi K, Motomura T, Mano Y, Uchiyama H, *et al.* **New method for assessing liver fibrosis based on acoustic radiation force impulse: a special reference to the difference between right and left liver**. *J Gastroenterol*. 2011;46(5):705-11.

[80] Uze G, Lutfalla G, Gresser I. **Genetic transfer of a functional human interferon alpha receptor into mouse cells: cloning and expression of its cDNA**. *Cell*. 1990;60(2):225-34.

[81] Velazquez L, Fellous M, Stark GR, Pellegrini S. **A protein tyrosine kinase in the interferon alpha/beta signaling pathway**. *Cell*. 1992;70(2):313-22.

[82] Wakita T, Pietschmann T, Kato T, Date T, Miyamoto M, Zhao Z, *et al.* **Production of infectious hepatitis C virus in tissue culture from a cloned viral genome**. *Nature medicine*. 2005;11(7):791-6.

[83] Webster DP, Klenerman P, Collier J, Jeffery KJ. **Development of novel treatments for hepatitis C**. *The Lancet Infectious diseases*. 2009;9(2):108-17.

[84] Yamamoto M, Sato S, Hemmi H, Hoshino K, Kaisho T, Sanjo H, *et al.* **Role of adaptor TRIF in the MyD88-independent toll-like**

receptor signaling pathway. *Science*. 2003;301(5633):640-3.

[85] Zeuzem S. **Interferon-based therapy for chronic hepatitis C: current and future perspectives**. *Nature clinical practice Gastroenterology & hepatology*. 2008;5(11):610-22.